Large but decreasing effect of ozone on the European carbon sink

Rebecca J Oliver[1], Lina M Mercado[1,2], Stephen Sitch[2], David Simpson[3,4], Belinda E Medlyn[5], Yan-Shih Lin[5], Gerd A Folberth[6]

[1] Centre for Ecology and Hydrology, Benson Lane, Wallingford, OX10 8BB, UK

[2] College of Life and Environmental Sciences, University of Exeter, EX4 4RJ, Exeter, UK

[3] EMEP MSC-W Norwegian Meteorological Institute, PB 43, NO-0313, Oslo, Norway

[4] Dept. Space, Earth & Environment, Chalmers University of Technology, Gothenburg, SE-41296 Sweden

[5] Hawkesbury Institute for the Environment, Western Sydney University, Locked Bag 1797, Penrith NSW 2751 Australia

[6] Met Office Hadley Centre, Exeter, UK.

Correspondence to: Rebecca Oliver (rfu@ceh.ac.uk)

26   **Abstract**

28   The capacity of the terrestrial biosphere to sequester carbon and mitigate climate change is governed by the ability

29   of vegetation to remove emissions of CO_2 through photosynthesis. Tropospheric O_3, a globally abundant and

30   potent greenhouse gas, is, however, known to damage plants, causing reductions in primary productivity. Despite

31   emission control policies across Europe, background concentrations of tropospheric O_3 have risen significantly

32   over the last decades due to hemispheric-scale increases in O_3 and its precursors. Therefore, plants are exposed to

33   increasing background concentrations, at levels currently causing chronic damage. Studying the impact of O_3 on

34   European vegetation at the regional scale is important for gaining greater understanding of the impact of O_3 on

35   the land carbon sink at large spatial scales. In this work we take a regional approach and update the JULES land-

36   surface model using new measurements specifically for European vegetation. Given the importance of stomatal

37   conductance in determining the flux of O_3 into plants, we implement an alternative stomatal closure

38   parameterization and account for diurnal variations in O_3 concentration in our simulations. We conduct our

39   analysis specifically for the European region to quantify the impact of the interactive effects of tropospheric O_3

40   and CO_2 on gross primary productivity (GPP) and land carbon storage across Europe. A factorial set of model

41   experiments showed that tropospheric O_3 can suppress terrestrial carbon uptake across Europe over the period

42   1901 to 2050. By 2050, simulated GPP was reduced by 4 to 9% due to plant O_3 damage and land carbon storage

43   by 3 to 7%. The combined physiological effects of elevated future CO_2 (acting to reduce stomatal opening) and

44   reductions in O_3 concentrations resulted in reduced O_3 damage in the future. This alleviation of O_3 damage by

45   CO_2 induced stomatal closure was around 1 to 2% for both land carbon and GPP, depending on plant sensitivity

46   to O_3. Reduced land carbon storage resulted from diminished soil carbon stocks consistent with the reduction in

47   GPP. Regional variations are identified with larger impacts shown for temperate Europe (GPP reduced by 10 to

48   20%) compared to boreal regions (GPP reduced by 2 to 8%). These results highlight that O_3 damage needs to be

49   considered when predicting GPP and land carbon, and that the effects of O_3 on plant physiology need to be

50   considered in regional land carbon cycle assessments.

51

52

53

54

55

56

57

58

1 Introduction

The terrestrial biosphere absorbs around 30% of anthropogenic CO_2 emissions and acts to mitigate climate change (Le Quéré et al., 2015). Early estimates of the European carbon balance suggest a terrestrial carbon sink of between 135 to 205 TgC yr^{-1} (Janssens et al., 2003). Schulze et al. (2009) determined a larger carbon sink of 274 TgC yr^{-1}, and more recent estimates suggest a European terrestrial sink of between 146 to 184 TgC yr^{-1} (Luyssaert et al., 2012). The carbon sink capacity of land ecosystems is dominated by the ability of vegetation to sequester carbon through photosynthesis and release it back to the atmosphere through respiration. Therefore, any change in the balance of these fluxes will alter ecosystem source-sink behaviour.

In recent decades much attention has focussed on the effects of rising atmospheric CO_2 on vegetation productivity (Ceulemans and Mousseau, 1994;Norby et al., 2005;Norby et al., 1999;Saxe et al., 1998). The Norby et al. (2005) synthesis of Free Air CO_2 Enrichment (FACE) experiments suggests a median stimulation (23 ± 2%) of forest NPP in response to a doubling of CO_2. Similar average increases (20%) were observed for C_3 crops, although this translated into smaller gains in biomass (17%) and crop yields (13%) (Long et al., 2006). Little attention, however, has been given to tropospheric ozone (O_3), a globally abundant air pollutant recognised as one of the most damaging pollutants for forests (Karlsson et al., 2007;Royal-Society, 2008;Simpson et al., 2014b). Tropospheric O_3 is a secondary air pollutant formed by photochemical reactions involving carbon monoxide (CO), volatile organic compounds (VOCs), methane (CH_4) and nitrogen oxides (NO_x) from both man-made and natural sources, as well as downward transport from the stratosphere and lightning which is a source of NO_x. The phytotoxic effects of O_3 exposure are shown to decrease vegetation productivity and biomass, with consequences for terrestrial carbon sequestration (Felzer et al., 2004;Loya et al., 2003;Mills et al., 2011b;Sitch et al., 2007). Few studies, however, consider the simultaneous effects of exposure to both gases, and few Earth-system models (ESMs) currently explicitly consider the role of tropospheric O_3 in terrestrial carbon dynamics (IPCC, 2013), both of which are important to understanding the carbon sequestration potential of the land-surface, and future carbon dynamics regionally and globally (Le Quéré et al., 2016;Sitch et al., 2015).

Due to increased anthropogenic precursor emissions over the industrial period, background concentrations of ground-level O_3 have risen (Vingarzan, 2004). Background O_3 is generally defined as the O_3 pollution present in a region that is not attributed to local anthropogenic sources (Vingarzan, 2004). O_3 levels at the start of the 20th century are estimated to be around 10 ppb for the site Montsouris Observatory near Paris, data for Arkona on the Baltic coast increased from ca. 15 ppb in the 1950s to 20-27 ppb by the early 1980s, and the Irish coast site Mace Head shows around 40 ppb by the year 2000 (Logan et al., 2012;Parrish et al., 2012). Present day annual average background O_3 concentrations reported in the review of Vingarzan (2004) show O_3 concentrations range between approximately 20 and 45 ppb, with the greatest increase occurring since the 1950s. Trends vary from site to site though, even on a decadal basis (Logan et al., 2012;Simpson et al., 2014b), depending, for example, on local/regional trends in precursor (especially NOx) emissions, elevation, and exposure to long-range transport of O_3. Nevertheless, there is some indication that background O_3 levels over the mid-latitudes of the Northern Hemisphere have continued to rise at a rate of approximately 0.5–2% per year, although not uniform (Vingarzan, 2004). As a result of controls on precursor emissions in Europe and North America, peak O_3 concentrations in

99   these regions have decreased or stabilised over recent decades (Cooper et al., 2014;Logan et al., 2012;Parrish et

100   al., 2012;Simpson et al., 2014b). Nevertheless, climate change may increase the frequency of weather events

101   conducive to peak O_3 incidents in the future (e.g. summer droughts and heat-waves (Sicard et al., 2013)), and may

102   increase biogenic emissions of the O_3-precursors isoprene and NO_x, although such impacts are subject to great

103   uncertainty (Simpson et al., 2014b;Young et al., 2013;Young et al., 2009). Intercontinental transport of air

104   pollution from regions such as Asia are thought to contribute substantially to rising background O_3 concentrations

105   over the last decades (Cooper et al., 2010;Verstraeten et al., 2015). Northern Hemisphere background

106   concentrations of O_3 are now close to established levels for impacts on human health and the terrestrial

107   environment (Royal-Society, 2008). Therefore, although peak O_3 concentrations are in decline across Europe,

108   plants are exposed to increasing background levels, at levels currently causing chronic damage (Mills et al.,

109   2011b). Intercontinental transport means future O_3 concentrations in Europe will be partly dependent on how O_3

110   precursor emissions evolve globally (Auvray and Bey, 2005;Derwent et al., 2015).

111

112   Rising background O_3 concentrations impact agricultural yields and nutritional quality of major crops (Ainsworth

113   et al., 2012;Avnery et al., 2011), with consequences for global food security (Tai et al., 2014). Increasing

114   background levels of O_3 are damaging to ecosystem health and reduce the global land carbon sink (Arneth et al.,

115   2010;Sitch et al., 2007). Reduced uptake of carbon by plant photosynthesis due to O_3 damage allows more CO_2

116   to remain in the atmosphere. This effect of O_3 on plant physiology represents an additional climate warming to

117   the direct radiative forcing of O_3, a potent greenhouse gas (Collins et al., 2010;Sitch et al., 2007), the magnitude

118   of which, however, remains highly uncertain (IPCC, 2013).

119

120   Dry deposition of O_3 to terrestrial surfaces, primarily uptake by stomata on plant foliage and deposition on external

121   surfaces of vegetation (Fowler et al., 2001;Fowler et al., 2009), is a large sink for ground level O_3 (Wild,

122   2007;Young et al., 2013). On entry to sub-stomatal spaces, O_3 reacts with other molecules to form reactive oxygen

123   species (ROS). Plants can tolerate a certain level of O_3 depending on their capacity to scavenge and detoxify the

124   ROS (Ainsworth et al., 2012). Above this critical level, long-term chronic O_3 exposure reduces plant

125   photosynthesis and biomass accumulation (Ainsworth, 2008;Ainsworth et al., 2012;Matyssek et al., 2010a;Wittig

126   et al., 2007;Wittig et al., 2009), either directly through effects on photosynthetic machinery such as reduced

127   Rubisco content (Ainsworth et al., 2012;Wittig et al., 2009) and/or indirectly by reduced stomatal conductance

128   (g_s) (Kitao et al., 2009;Wittig et al., 2007), alters carbon allocation to different pools (Grantz et al., 2006;Wittig

129   et al., 2009), accelerates leaf senescence (Ainsworth, 2008;Nunn et al., 2005;Wittig et al., 2009) and changes plant

130   susceptibility to biotic stress factors (Karnosky et al., 2002;Percy et al., 2002).

131

132   The response of plants to O_3 is very wide ranging as reported in the literature from different field studies. The

133   Wittig et al. (2007) meta-analysis of temperate and boreal tree species showed raised O_3 concentrations

134   significantly reduced leaf level light saturated net photosynthetic uptake (-19%, range: -3% to -28% at a mean O_3

135   concentration of 85 ppb) and g_s (-10%, range: +5% to -23% at a mean O_3 concentration of 91 ppb) in both

136   broadleaf and needle leaf tree species. In the Feng et al. (2008) meta-analysis of wheat, O_3 reduced aboveground

137   biomass (-18% at a mean O_3 concentration of 70 ppb) photosynthetic rate (-20% at a mean O_3 concentration of 73

138   ppb) and g_s (-22% at a mean O_3 concentration of 79 ppb). One of few long-term field based O_3 exposure studies

139   (AspenFACE) showed that after 11 years of exposing mature trees to O_3 (mean O_3 concentration of 46 ppb), O_3
140   decreased ecosystem carbon content (-9%), and decreased NPP (-10%), although the O_3 effect decreased through
141   time (Talhelm et al., 2014). Zak et al. (2011) showed this was partly due to a shift in community structure as O_3-
142   tolerant species, competitively inferior in low O_3 environments, out competed O_3-sensitivie species. GPP was
143   reduced (-12% to -19%) at two Mediterranean ecosystems exposed to O_3 (ranging between 20 to 72 ppb across
144   sites and through the year) studied by Fares et al. (2013). Biomass of mature beech trees was reduced (-44%) after
145   8 years of exposure to O_3 (~150 ppb) (Matyssek et al., 2010a). After 5 years of O_3 exposure (ambient +20 to +40
146   ppb) in a semi-natural grassland, annual biomass production was reduced (-23%), and in a Mediterranean annual
147   pasture O_3 exposure significantly reduced total aboveground biomass (up to -25%) (Calvete-Sogo et al., 2014).
148   However, these were empirical studies at individual sites, and these focus on O_3 effects on plant physiology and
149   productivity, but do not quantify the impact on the land carbon sink. Modelling studies are needed to scale site
150   observations to the regional and global scales. Models generally suggest that plant productivity and carbon
151   sequestration will decrease with O_3 pollution, though the magnitudes vary. For example, based on a limited dataset
152   to parameterise plant O_3 damage for a global set of plant functional types, Sitch et al. (2007) predicted a decline
153   in global GPP of 14 to 23% by 2100. A second study by Lombardozzi et al. (2015) predicted a 10.8% decrease of
154   present-day (2002-2009) GPP globally. Here we take a regional approach and take advantage of the latest
155   measurements showing changes in plant productivity with accumulated exposure to O_3 specifically for a range of
156   European vegetation from different regions (CLRTAP 2017) with which to calibrate the JULES model for plant
157   sensitivity to O_3, and conduct our analysis specifically for the European region.

158

159   Understanding the response of plants to elevated tropospheric O_3 is challenged by the large variation in O_3
160   sensitivity both within and between species (Karnosky et al., 2007;Kubiske et al., 2007;Wittig et al., 2009).
161   Additionally, other environmental stresses that affect stomatal behaviour will affect the rate of O_3 uptake and
162   therefore the response to O_3 exposure, such as high temperature, drought and changing concentrations of
163   atmospheric CO_2 (Mills et al., 2016;Fagnano et al., 2009;Kitao et al., 2009;Löw et al., 2006). Increasing
164   concentrations of atmospheric CO_2, for example, are suggested to provide some protection against O_3 damage by
165   causing stomata to close (Harmens et al., 2007;Wittig et al., 2007), however the long-term effects of CO_2
166   fertilisation on plant growth and carbon storage remain uncertain (Baig et al., 2015;Ciais et al., 2013). Further, in
167   some studies, stomata have been shown to respond sluggishly, losing their responsiveness to environmental
168   stimuli with exposure to O_3 which can lead to higher O_3 uptake, increased water-loss and therefore greater
169   vulnerability to environmental stresses such as drought (Mills et al., 2016;Mills et al., 2009;Paoletti and Grulke,
170   2010;Wilkinson and Davies, 2009).

171

172   Given the critical role g_s plays in the uptake of both CO_2 and O_3, we use an alternative representation and
173   parameterisation of g_s in JULES by implementing the Medlyn *et al.* (2011) g_s formulation. This model is based
174   on the optimal theory of stomatal behaviour and has advantages over the current JULES g_s formulation of Jacobs
175   (1994) including i) a single parameter (g_1) compared to two parameters in Jacobs (1994), ii) the g_1 parameter is
176   related to the water-use strategy of vegetation and is easier to parameterise with commonly measured leaf or
177   canopy level observations of photosynthesis, g_s and humidity, and (iii) values of g_1 are available for many
178   different plant functional types (PFTs) derived from a global data set of leaf-level measurements (Lin et al., 2015).

179

180   The main objective of this work is to assess the impact of historical and projected (1901 to 2050) changes in

181   tropospheric O_3 and atmospheric CO_2 concentration on predicted GPP and the land-carbon sink for Europe.

182   These are the two greenhouse gases that directly affect plant photosynthesis and g_s. We use a factorial suite of

183   model experiments, using the Joint UK land environment simulator (JULES) (Best et al., 2011;Clark et al.,

184   2011), the land-surface model of the UK Earth System Model (UKESM) (Collins et al., 2011) to simulate plant

185   O_3 uptake and damage, and to investigate the impact of both O_3 and CO_2 on plant water-use and carbon uptake.

186   In this work, the JULES model is re-calibrated using the latest observations of vegetation sensitivity to O_3, with

187   the addition of a separate parameterisation for temperate/boreal regions versus the Mediterranean. The O_3

188   sensitivity of each PFT in JULES was re-calibrated for both a high and low sensitivity to account for uncertainty

189   in the O_3 response, in part due to the observed variation in O_3 sensitivity between species. This includes O_3

190   sensitivities for agricultural crops (wheat – high sensitivity) versus natural grassland (low sensitivity), with

191   separate sensitivities for Mediterranean grasslands. For forests JULES is parameterised with O_3 sensitivities for

192   broadleaf and needle leaf trees (with a high and low O_3 sensitivity for both), with separate sensitivities (high and

193   low) for Mediterranean broadleaf species. We make a separate distinction for the Mediterranean region where

194   possible because the work of Büker et al. (2015) showed that the sensitivity of dominant Mediterranean trees to

195   O_3 is different to temperate species. In addition, we introduce an alternative g_s scheme into JULES as described

196   above. JULES is forced with spatially varying daily O_3 concentrations from a high resolution atmospheric

197   chemistry model for Europe that are disaggregated to hourly concentrations, therefore our simulations account

198   for diurnal variations in O_3 concentration and O_3 responses allowing for improved estimates of O_3 uptake by

199   vegetation. We do not attempt to make a full assessment of the carbon cycle of Europe, instead we target O_3

200   damage, which is currently a missing component in earlier carbon cycle assessments (Le Quéré et al.,

201   2017;Sitch et al., 2015). To this end, we prescribe changing O_3 and CO_2 concentrations from 1901 to 2050, but

202   use a fixed pre-industrial climate. We acknowledge the use of a 'fixed' pre-industrial climate omits the additional

203   uncertainty of the interaction between climate change and g_s which will affect the rate of O_3 uptake and

204   therefore O_3 concentrations. In addition, using uncoupled chemistry and climate is a further source of

205   uncertainty. To understand the impact of these complex feedback mechanisms is an important area for future

206   work, but in the current study our aim is to isolate the physiological response of plants to both O_3 and CO_2, and

207   determine the sensitivity of predicted GPP and the land carbon sink to this process, as the impact of O_3 on the

208   land carbon sink currently remains largely unknown at large spatial scales for Europe.

209

210

211

212   **2 Methods**

213

214   **2.1 Representation of O_3 effects in JULES**

215

216   JULES calculates the land-atmosphere exchanges of heat, energy, mass, momentum and carbon on a sub-daily

217   time step, and includes a dynamic vegetation model (Best et al., 2011;Clark et al., 2011;Cox, 2001). This work

218   uses JULES version 3.3 (http://www.jchmr.org) at 0.5º x 0.5º spatial resolution and hourly model time step, the

219 spatial domain is shown in Fig. S1. JULES has a multi-layer canopy radiation interception and photosynthesis

220 scheme (10 layers in this instance) that accounts for direct and diffuse radiation, sun fleck penetration through the

221 canopy, inhibition of leaf respiration in the light and change in photosynthetic capacity with depth into the canopy

222 (Clark et al., 2011;Mercado et al., 2009). Soil water content also affects the rate of photosynthesis and g_s. It is

223 modelled using a dimensionless soil water stress factor, β, which is related to the mean soil water concentration

224 in the root zone, and the soil water contents at the critical and wilting point (Best *et al*., 2011).

225

226 To simulate the effects of stomatal O_3 deposition on vegetation productivity and water use, JULES uses the flux-

227 gradient approach of Sitch *et al*., (2007), modified to include non-stomatal deposition following Tuovinen et al.

228 (2009). A similar approach is taken by Franz et al. (2017) in the OCN model, however plant O_3 damage is a

229 function of accumulated O_3 exposure over time. In JULES, plant O_3 damage is instantaneous, because the impact

230 of cumulative O_3 exposure on plant productivity has already been calibrated with observations (described below).

231 JULES uses a coupled model of g_s and photosynthesis, the potential net photosynthetic rate (A_p, mol CO_2 m^{-2} s^{-1})

232 is modified by an 'O_3 uptake' factor (F, the fractional reduction in photosynthesis), so that the actual net

233 photosynthesis (A_{net}, mol CO_2 m^{-2} s^{-1}) is given by equation 1 (Clark *et al.,* 2011, Sitch *et al.,* 2007). Because of the

234 relationship between these two fluxes, the direct effect of O_3 damage on photosynthetic rate also leads to a

235 reduction in g_s. An alternative approach was taken by Lombardozzi et al. (2012) in the CLM model where

236 photosynthesis and g_s are decoupled, so that O_3 exposure affects carbon assimilation and transpiration

237 independently. In JULES, changes in atmospheric CO_2 concentration also affect photosynthetic rate and g_s,

238 consequently the interactive effects of changing concentrations of both CO_2 and O_3 is allowed for.

239

240 $$A_{net} = A_P F \qquad\qquad\qquad (1)$$

241

242 The O_3 uptake factor (F) is defined as:

243

244 $$F = 1 - a * max[F_{O3} - F_{O3crit}, 0.0] \qquad\qquad\qquad (2)$$

245

246 F_{O3} is the instantaneous leaf uptake of O_3 (nmol m^{-2} s^{-1}), F_{O3crit} is a PFT-specific threshold for O_3 damage (nmol

247 m^{-2} PLA s^{-1}, projected leaf area), and '*a*' is a PFT-specific parameter representing the fractional reduction of

248 photosynthesis with O_3 uptake by leaves. Following Tuovinen et al. (2009), the flux of O_3 through stomata, F_{O3},

249 is represented as follows:

250

251 $$F_{O3} = O_3 \left(\frac{g_b\left(\frac{g_l}{K_{O3}}\right)}{g_b + \left(\frac{g_l}{K_{O3}}\right) + g_{ext}} \right) \qquad\qquad\qquad (3a)$$

252

253 O_3 is the molar concentration of O_3 at reference (canopy) level (nmol m^{-3}), g_b is the leaf-scale boundary layer

254 conductance (m s^{-1}, eq 3b), g_l is the leaf conductance for water (m s^{-1}), K_{O3} accounts for the different diffusivity of

255 ozone to water vapour and takes a value of 1.51 after Massman (1998), and g_{ext} is the leaf-scale non-stomatal

256 deposition to external plant surfaces (m s^{-1}) which takes a constant value of 0.0004 m s^{-1} after Tuovinen et al.

257 (2009). The leaf-level boundary layer conductance (g_b) is calculated as in Tuovinen *et al*. (2009)

258

259   $g_b = \alpha L d^{-1/2} U^{-1/2}$ (3b)

260

261   α is a constant (0.0051 m s$^{-1/2}$), Ld is the cross-wind leaf dimension (m) defined per PFT as 0.05 for trees, 0.02

262   for grasses (C$_3$ and C$_4$) and 0.04 for shrubs, U is wind speed at canopy height (m s^{-1}). The rate of O$_3$ uptake is

263   dependent on g_s, which is dependent on photosynthetic rate. Given g_s is a linear function of photosynthetic rate in

264   JULES (Clark et al., 2011), from eq 1 it follows that:

265

266   $g_s = g_l F$ (4)

267

268   The O$_3$ flux to stomata, F_{O3}, is calculated at leaf level and then scaled to each canopy layer differentiating sunlit

269   and shaded leaf photosynthesis, and finally summed up to the canopy level. Because the photosynthetic capacity,

270   photosynthesis and therefore g_s decline with depth into the canopy, this in turn affects O$_3$ uptake, with the top leaf

271   level contributing most to the total O$_3$ flux and the lowest level contributing least.

272

273   **2.2 Calibration of O$_3$ uptake model**

274

275   Here we use the latest literature on flux based O$_3$ dose-response relationships derived from observed field data

276   across Europe (CLRTAP, 2017) to determine the key PFT-specific O$_3$ sensitivity parameters in JULES (*a* and

277   *Fo$_{3crit}$*). Synthesis of information expressed as O$_3$ flux based dose-response relationships derived from field

278   experiments is carried out by The United Nations Convention on Long-Range Transboundary Air Pollution

279   (CLRTAP Convention), this information is then used as a policy tool to inform emission reduction strategies in

280   Europe to improve air quality (CLRTAP, 2017;Mills et al., 2011a). Derivation of O$_3$ flux based dose-response

281   relationships for different vegetation types uses the accumulated stomatal O$_3$ flux above a threshold (often referred

282   to as the phytotoxic O$_3$ dose above a threshold of 'y' i.e. POD$_y$) as the dose metric, and the percentage change in

283   biomass as the response metric (Emberson et al., 2007;Karlsson et al., 2007). We use these observation based O$_3$

284   dose-response relationships to calibrate each JULES PFT for sensitivity to O$_3$ using available relationships for the

285   closest matching vegetation type. For JULES, *Fo$_{3crit}$* is the threshold for O$_3$ damage, and values for this parameter

286   are taken from the O$_3$ dose-response relationships as the POD$_y$ value (see CLRTAP, 2017 and Buker et al. 2015

287   for derivation of POD$_y$ values). The actual sensitivity to O$_3$ is determined by the slope of the O$_3$ dose-response

288   relationship, i.e. how much biomass changes with accumulated stomatal uptake of O$_3$ above the damage threshold,

289   this relates to the parameter *a* in JULES. The parameter '*a*' is a PFT-specific parameter representing the fractional

290   reduction of photosynthesis with O$_3$ uptake by leaves. Values for this parameter are found for each PFT by running

291   JULES with different values of '*a*', which alter the instantaneous photosynthetic rate, but then calculating the

292   accumulated stomatal flux of O$_3$ and the change in productivity, until the slope of this relationship produced by

293   the JULES simulations matches that of the O$_3$ dose-response relationships derived from observations. Essentially

294   we calibrate each JULES PFT for sensitivity to O$_3$ by reproducing the observation-based O$_3$ dose-response

295   relationships.

296

297   Each PFT was calibrated for high and low plant O_3 sensitivity to account for uncertainty in the sensitivity of

298   different plant species to O_3, using the approach of Sitch *et al*., (2007). Therefore, when using our results to assess

299   the impact of O_3 at the land surface, we are able to provide a range in our estimates to help address some of the

300   uncertainty in the O_3 response of different vegetation types. In addition, where possible owing to available data,

301   a distinction was made for Mediterranean regions. This was because the work of Büker et al. (2015) showed that

302   different O_3 dose-response relationships are needed to describe the O_3 sensitivity of dominant Mediterranean trees.

303   For the C_3 herbaceous PFT, the dominant land cover type across the European domain in this study (Fig. S2), the

304   high plant O_3 sensitivity was calibrated against observations for wheat to give a representation of agricultural

305   regions and wheat is one of the most sensitive grasses to O_3 (Fig. S3, Table S1). For the low plant O_3 sensitivity

306   JULES was calibrated against the dose-response function for natural grassland to give a representation of natural

307   grassland and this vegetation has a much lower sensitivity to O_3 damage, for the Mediterranean region we used a

308   function for Mediterranean natural grasslands, all taken from CLRTAP (2017) (Fig. S3, Table S1). Tree/shrub

309   PFTs were calibrated against observed O_3 dose-response functions for the high plant O_3 sensitivity: broadleaf

310   trees (temperate/boreal) = Birch/Beech dose-response relationship, broadleaf trees (Mediterranean) = deciduous

311   oaks dose-response relationship, needle leaf trees = Norway spruce dose-response relationship, shrubs =

312   Birch/Beech dose-response relationship, all from CLRTAP (2017) (Fig. S3, Table S1). Data on O_3 dose-response

313   relationships for different vegetation types is very limited, therefore for the low plant O_3 sensitivity calibration for

314   trees/shrubs we assumed a 20% decrease in sensitivity to O_3 based on the difference in sensitivity between high

315   and low sensitive tree species in the Karlsson et al. (2007) study. Due to limitations in data availability, the shrub

316   parameterisation uses the observed dose-response functions for broadleaf trees. Similarly, the parameterisation

317   for C_4 herbaceous uses the observed dose-responses for C_3 herbaceous, however the fractional cover of C_4 herbs

318   across Europe is low (Fig. S2), so this assumption affects a very small percentage of land cover.

319

320   To calibrate the JULES O_3 uptake model, JULES was run across Europe forced using the WFDEI observational

321   climate dataset (Weedon, 2013) at 0.5º X 0.5º spatial and three hour temporal resolution. JULES uses interpolation

322   to disaggregate the forcing data down from 3 hours to an hourly model time step. The model was spun-up over

323   the period 1979 to 1999 with a fixed atmospheric CO_2 concentration of 368.33 ppm (1999 value from Mauna Loa

324   observations (Tans and Keeling, 2014)). Zero tropospheric ozone concentration was assumed for the control

325   simulation, for the simulations with O_3, spin-up used spatially explicit fields of present day O_3 concentration

326   produced using the UK Chemistry and Aerosol (UKCA) model with standard chemistry from the run evaluated

327   by O'Connor et al. (2014). A fixed land cover map was used based on IGBP (International Geosphere-Biosphere

328   Programme) land cover classes (IGBP-DIS), therefore as the vegetation distribution was fixed and the calibration

329   was not looking at carbon stores, a short spin-up was adequate to equilibrate soil temperature and soil moisture.

330   JULES was then run for the year 2000 with a corresponding CO_2 concentration of 369.52 ppm (from Mauna Loa

331   observations (Tans and Keeling, 2014)) and monthly fields of spatially explicit tropospheric O_3 (O'Connor et al.,

332   2014) as necessary.

333

334   Calibration was performed using four simulations: with i) zero tropospheric O_3 concentration, this was the control

335   simulation (control), ii) tropospheric O_3 at current ambient concentration (O3), iii) ambient +20 ppb (O3+20) and

336   iv) ambient +40 ppb (O3+40). The different O_3 simulations (i.e. O3, O3+20 and O3+40) were used to capture the

337   range of O_3 conditions in the data used in the observation-based O_3 dose-response relationships used in this study

338   for calibration, often data were from experiments using artificially manipulated conditions of ambient + 40 ppb

339   O_3 for example. For each JULES O_3 simulation, the value of F_{O3crit} was taken from the vegetation specific O_3

340   dose-response relationship as the threshold O_3 concentration above which damage to vegetation occurs. An initial

341   estimate of the parameter 'a' was used, then for each PFT and each simulation, hourly estimates of NPP (our

342   proxy for biomass – although not identical they are related) and O_3 uptake in excess of F_{O3crit} were accumulated

343   over a PFT dependent accumulation period. The accumulation periods were ~6 months for broadleaf trees and

344   shrubs, all year for needle leaf trees, and ~3 months for herbaceous species, through the growing season, following

345   guidelines in CLRTAP (2017). Additionally, in accordance with the methods used in the CLRTAP (2017) that

346   describe how the O_3 dose-response relationships are derived from observations, we use the stomatal O_3 flux per

347   projected leaf area to top canopy sunlit leaves. The percentage change in total NPP was calculated for each O_3

348   simulation and plotted against the cumulative uptake of O_3 over the PFT-specific accumulation period. The linear

349   regression of this relationship was calculated, and slope and intercept compared against the slope and intercept of

350   the observed dose-response relationships. Values of the parameter 'a' were adjusted, and the procedure repeated

351   until the linear regression through the simulation points matched that of the observations (Fig. S3, Table S1).

352

353   **2.3 Representation of stomatal conductance and site level evaluation**

354

355   In JULES, g_s (m s^{-1}) is represented following the closure proposed by (Jacobs, 1994):

356

357    $g_s = 1.6RT_l \frac{A_{net}\beta}{c_a - c_i}$ (5)

358

359   In this parameterisation, c_i is unknown and in the default JULES model is calculated as in equation 6, hereafter

360   called JAC:

361

362    $c_i = (c_a - c_*)f0\left(1 - \frac{dq}{dq_{crit}}\right) + c_*$ (6)

363

364   β is a soil moisture stress factor, the factor 1.6 accounts for g_s being the conductance for water vapour rather than

365   CO_2, R is the universal gas constant (J K^{-1} mol^{-1}), T_l is the leaf surface temperature (K), c_a and c_i (both Pa) are the

366   leaf surface and internal CO_2 partial pressures, respectively, c_* (Pa) is the CO_2 photorespiration compensation

367   point, dq is the humidity deficit at the leaf surface (kg kg^{-1}), dq_{crit} (kg kg^{-1}) and f_0 are PFT specific parameters

368   representing the critical humidity deficit at the leaf surface, and the leaf internal to atmospheric CO_2 ratio (c_i/c_a)

369   at the leaf specific humidity deficit (Best *et al.* 2011), values are shown is Table S1.

370

371   In this work, we replace equation 6 with the closure described in Medlyn et al. (2011), using the key PFT specific

372   model parameter g_l (kPa$^{0.5}$), and dq is expressed in kPa, shown in eq 7, hereafter called MED:

373

374    $c_i = c_a\left(\frac{g_1}{g_1 + \sqrt{dq}}\right)$ (7)

375

376   PFT specific values of the g_l parameter were derived for European vegetation from the data base of Lin et al.

377   (2015) and are shown in Table S1. The g_l parameter represents the sensitivity of g_s to the assimilation rate, i.e.

378   plant water use efficiency, and was derived as in Lin et al. (2015) by fitting the Medlyn *et al.*, (2011) model to

379   observations of g_s, photosynthesis, and VPD, assuming an intercept of zero.

380

381   The impact of g_s model formulation (JAC versus MED) on simulated water, O_3, carbon and energy fluxes is

382   compared for two contrasting grid points - wet (low soil moisture stress) and dry (high soil moisture stress) in the

383   European domain. JULES was spun-up for 20 years (1979-1999) at two grid points in central Europe representing

384   a wet (low soil moisture stress, lat: 48.25; lon:, 5.25) and a dry site (high soil moisture stress, lat: 38.25; lon:, -

385   7.75). The modelled soil moisture stress factor (*fsmc*) at the wet site ranged from 0.8 to 1.0 over the year 2000

386   (1.0 indicates no soil moisture stress), and at the dry site *fsmc* steadily declined from 0.8 at the start of the year to

387   0.25 by the end of the summer. The WFDEI meteorological forcing dataset was used (Weedon, 2013), along with

388   atmospheric CO_2 concentration for the year 1999 (368.33 ppm), and either no O_3 (i.e. the O_3 damage model was

389   switched off) for the control simulations, or spatially explicit fields of present day O_3 concentration produced

390   using the UK Chemistry and Aerosol (UKCA) model from the run evaluated by O'Connor et al. (2014) for the

391   simulations with O_3. Following the spin-up period, JULES was run for one year (2000) with corresponding

392   atmospheric CO_2 concentration, and tropospheric O_3 concentrations as described above. The control and O_3

393   simulations were performed for both JAC and MED model formulations. Land cover for the spin-up and main run

394   was fixed at 20% for each PFT. For the simulations including O_3 damage, the high plant O_3 sensitivity

395   parameterisation was used. The difference between these simulations was used to assess the impact of g_s model

396   formulation on the leaf level fluxes of carbon and water. We calculate and report (results section 3.1) the difference

397   in mean annual water-use that results from the above simulations using the different g_s models. For each day of

398   the simulation we calculate the percentage difference in water-use between the two simulations, we then calculate

399   the mean and standard deviation over the year to give the annual mean leaf-level water-use.

400

401   Site level evaluation of the two g_s models compared to FLUXNET observations was carried out to evaluate the

402   seasonal cycles of latent and sensible heat using the two g_s models JAC and MED compared to observations.

403   Seven Fluxnet towers were selected to represent a range of land cover types as shown in Table S2. JULES was

404   setup for each site using observed site-level hourly meteorology, and the vegetation cover was prescribed

405   according to the fractional covers of the different JULES surface types shown in Table S2. Following a spin-up

406   period, simulations were run at each site for the years shown in Table S2.

407

408   **2.4 Model simulations for Europe**

409

410   **2.4.1 Forcing datasets**

411

412   We used the WATCH meteorological forcing data set (Weedon et al., 2010;Weedon et al., 2011) at 0.5º x 0.5º

413   spatial and three hour temporal resolution for our JULES simulations. JULES interpolates this down to an hourly

414 model time step. For this study, the climate was kept constant by recycling over the period 1901 to 1920, to allow
415 us to focus on the impact of O_3, CO_2 and their interactive effects.

416

417 JULES was run with prescribed annual mean atmospheric CO_2 concentrations. Pre-industrial global CO_2
418 concentrations (1900 to 1960) were taken from Etheridge et al. (1996), 1960 to 2002 were from Mauna Loa
419 (Keeling and Whorf, 2004), as calculated by the Global Carbon Project (Le Quéré et al., 2016), and 2003-2050
420 were based on the IPCC SRES A1B scenario and were linearly interpolated to gap fill missing years (Fig. 1).

421

422 JULES was run including dynamic vegetation with a land cover mask giving the fraction of agriculture in each
423 0.5º x 0.5º grid cell based on the Hurtt et al. (2011) land cover database for the year 2000. The agricultural mask
424 is fixed and does not change over the simulation period. This means that whilst the model is allowed to evolve its
425 own vegetation cover outside of the agricultural mask, within the mask only C_3/C_4 herbaceous PFTs are allowed
426 to grow, with no competition from other PFTs. Therefore, through the simulation period, regions of agriculture
427 are maintained as such and not out-competed by forests for example, allowing for a more accurate representation
428 of the land cover of Europe in the model. No form of land management is simulated (i.e. no crop harvesting,
429 ploughing, rotation or grazing), growth and leaf area index (LAI) are determined by resource availability and
430 phenology. Outside of the agricultural mask, dynamic vegetation means that grid cell PFT coverage and LAI are
431 the result of resource availability, phenology and simulated competition. Across the model domain, simulated
432 mean annual LAI was dominantly within the range of 2 to 5 m^2/m^2 (Fig. S4 and S5). Following a full spin-up
433 period (to ensure equilibrium vegetation, carbon and water states), there was no significant change in the fractional
434 cover of each PFT over the simulation period (1901 - 2050). By 2050, increases in boreal forest cover occurred,
435 but this was less than 2% and limited to very small areas, given this small change we show just the land cover for
436 2050 in Fig. S2.

437

438 Tropospheric O_3 concentration was produced by the EMEP MSC-W model at 0.5º x 0.5º (Simpson et al., 2012),
439 driven with meteorology from the regional climate model RCA3 (Kjellström et al., 2011;Samuelsson et al., 2011),
440 which provides a downscaling of the ECHAM A1B-r3 (simulation 11 of Kjellström *et al.*, 2011). This setup
441 (EMEP+RCA3) is also used by Langner et al. (2012a), Simpson et al. (2014a), Tuovinen et al. (2013), Franz et
442 al. (2017) and Engardt et al. (2017), where further details and model evaluation can be found. Unfortunately, the
443 3-dimensional RCA3 data needed by the EMEP model was not available prior to 1960, but as in Engardt et al.
444 (2017) the meteorology of 1900-1959 had to be approximated by assigning random years from 1960 to 1969. This
445 procedure introduces some uncertainty of course, although Langner et al. (2012b) show that for the period 1990
446 to 2100 it is emissions change, rather than meteorological change, that drives modelled O_3 concentrations. The
447 emissions scenarios for 1900-2050 merge data from the International Institute of Applied System Analysis
448 (IIASA) for 2005-2050 (the so-called ECLIPSE 4a scenario), recently revised EMEP data for 1990, and a scaling
449 back from 1990 to 1900 using data from Lamarque et al. (2013). The trend in emissions of the major O_3 precursors
450 NO_x, NMVOC and Isoprene are shown from 1900 to 2050 over Europe in Fig. S6. Isoprene emissions are not
451 inputs to the EMEP model, but rather calculated at each time-step using temperature, radiation, and land-cover
452 specific emission factors (Simpson et al., 2012). Changes in the assumed background concentration of CH_4 (from
453 RCP6.0) (van Vuuren et al., 2011) are also shown in Fig. S6. Engardt et al. (2017) show the trend in emissions of

454   SO$_2$ and NH$_3$ from 1900 to 2050 over Europe. The EMEP model accounts for changes in BVOC emissions as a

455   result of predicted ambient temperature changes.

456

457   O$_3$ concentrations from EMEP MSC-W were calculated at canopy height for two land-cover categories: forest

458   and grassland (Fig. S7 and Fig. S8), which are taken as surrogates for high and low vegetation, respectively. These

459   canopy-height specific concentrations allow for the large gradients in O$_3$ concentration that can occur in the lowest

460   10s of metres, giving lower O$_3$ for grasslands than seen at e.g. 20 m in a forest canopy (Gerosa et al., 2017;Simpson

461   et al., 2012;Tuovinen et al., 2009). These canopy level O$_3$ concentrations are used as input to JULES, using the

462   EMEP O$_3$ concentrations for forest for the forest JULES PFTs (broadleaf/needle leaf tree and shrub), and the

463   EMEP O$_3$ concentrations for grassland for the grass/herbaceous JULES PFTs (C$_3$ and C$_4$). This study used daily

464   mean values of tropospheric O$_3$ concentration from EMEP disaggregated down to the hourly JULES model time-

465   step. The daily mean O$_3$ forcing was disaggregated to follow a mean diurnal profile of O$_3$, this was generated from

466   hourly O$_3$ output from EMEP MSC-W for the two land cover categories (forest and grassland as described above)

467   across the same model domain. O$_3$ concentrations follow a diurnal cycle and peak during the day, therefore

468   accounting for the diurnal variation in O$_3$ concentrations allows for a more realistic estimation of O$_3$ uptake.

469

470   Figure 1 shows large increases in tropospheric O$_3$ from pre-industrial to present day (2001), this is in line with

471   modelling studies (Young et al., 2013) and site observations (Derwent et al., 2008;Logan et al., 2012;Parrish et

472   al., 2012), and is predominantly a result of increasing anthropogenic emissions (Young et al., 2013). Figures S7

473   and S8 show this large increase in ground-level O$_3$ concentrations from 1901 to 2001 occurs in all seasons. Present

474   day O$_3$ concentration show a strong seasonal cycle, with a spring/summer peak in concentrations in the mid-

475   latitudes of the Northern Hemisphere (Derwent et al., 2008;Parrish et al., 2012;Vingarzan, 2004). Seasonal cycles

476   have been changing over the past decades however, attributed to changes in NO$_x$ and other emissions, as well as

477   changes in transport patterns (Parrish et al., 2013). These changes will likely continue in future as emissions and

478   meteorological factors impact photo-chemical O$_3$ production and transport patterns. Indeed, the O$_3$ concentrations

479   used in the simulations in this study show increased O$_3$ levels in winter and in some regions in autumn and spring

480   in 2050 compared to present day, this may be due to reduced titration of O$_3$ by NO as a result of reduced NO$_X$

481   emissions in the future (Royal Society, 2008). Summer O$_3$ concentrations are lower in 2050 however, compared

482   to 2001.

483

484
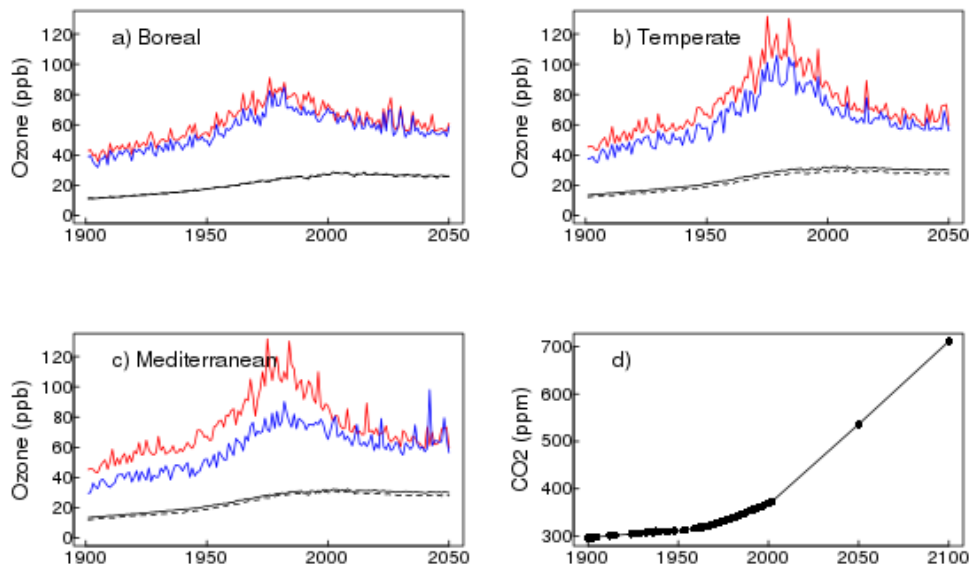
485

486 **Figure 1.** Regional time series of canopy height O_3 (ppb) forcing from EMEP a) to c), and d) global atmospheric

487 CO_2 (ppm) concentration (this does not vary regionally; black dots show data points, the black line shows

488 interpolated points). Each panel for the O_3 forcing shows the regional annual average (woody PFTs, black solid

489 line; herbaceous PFTs, black dashed line) and the annual maximum O_3 concentration above: woody PFTs (red)

490 and herbaceous PFTs (blue).

491

492 **2.4.2 Spin up and factorial experiments**

493

494 JULES was spun-up by recycling the climate from the early part of the twentieth century (1901 to 1920) using

495 atmospheric CO_2 (296.1 ppm) and O_3 concentrations from 1901 (Fig. S7 & Fig. S8). Model spin-up was 2000

496 years by which point the carbon pools and fluxes were in steady state with zero mean net land – atmosphere CO_2

497 flux. We performed the following transient simulations for the period 1901 to 2050 with continued recycling of

498 the climate as used in the spin-up, for both high and low plant O_3 sensitivities:

499

500 • **run_O3** : Fixed 1901 CO_2, Varying O_3

501 • **run_CO2** : Varying CO_2, Fixed 1901 O_3

502 • **run_both_CO2+O3** : Varying CO_2, Varying O_3

503

504 We use these simulations to investigate the direct effects of changing atmospheric CO_2 and O_3 concentrations,

505 individually and combined, on plant water-use, GPP and the land C sink through the twentieth century and into

506 the future, specifically over three time periods: historical (1901-2001), future (2001-2050) and over the full time

507 series (1901-2050). For each time period we calculate the difference between the decadal means calculated at the

508 start and end of the analysis period for each variable of interest. Therefore our results report the change in GPP,

509 for example, over the analysis period. For each variable analysed (GPP, NPP, vegetation carbon, soil carbon, total

510 land carbon and *gs*), we use the mean over 10 years to represent each time period, e.g. the mean over 2040 to 2050

511 is what we call 2050, 1901 to 1910 is what we refer to as 1901. The difference between the simulations gives the

512 effect of O_3 and CO_2 either separately or in combination over the different time periods. We look at the percentage

513   change due to either O_3 at pre-industrial CO_2 concentration (i.e. without the additional effect of atmospheric CO_2

514   on stomatal behaviour – run_O3), CO_2 (at fixed pre-industrial O_3 concentration, run_CO2) or the combined effect

515   of both gases (run_both_CO2+O3), e.g. 100 * (varO$_3$[2050] – varO$_3$[1901]) / varO$_3$[1901] gives the O_3 effect (at

516   fixed CO_2) over the full experimental period. The meteorological forcing is prescribed in these simulations and is

517   therefore the same between the model runs. Other climate factors, such as VPD, temperature and soil moisture

518   availability are accounted for in our simulations, but our analysis isolates the effects of O_3, CO_2 and O_3 + CO_2.

519   We also use paired t-test to determine statistically significant differences between the different (high and low)

520   plant O_3 sensitivities.

521

522   **2.4.3 Evaluation**

523   To evaluate our JULES simulations we compare mean GPP from 1991 to 2001 for each of the JULES scenarios

524   and both high and low plant O_3 sensitivities against the observation based globally extrapolated Flux Network

525   model tree ensemble (MTE) (Jung et al., 2011). We use paired t-test to determine statistically significant

526   differences in the mean responses.

527

528   **3 Results**

529

530   **3.1 Impact of g$_s$ model formulation and site level evaluation**

531

532   The impact of g_s model on simulated g_s is shown for the site with low soil moisture stress (wet site, Fig. 2). For

533   the broadleaf tree and C_3 herbaceous PFT, the MED model simulates a larger conductance compared to the JAC

534   model. In other words, with the MED model these two PFTs are parameterised with a less conservative water use

535   strategy, which, for the grid point shown in Fig. 2, increased the annual mean water use by 35% (±29%) and 45%

536   (±32%), respectively. In contrast, the needle leaf tree, C_4 herbaceous and shrub PFTs are parameterised with a

537   more conservative water use strategy with the MED model, and the mean annual g_s was decreased by 13% (±12%),

538   27% (±10%) and 36% (±13%), respectively, compared to the JAC model. This comparison was also done for a

539   dry site (high soil moisture stress), and similar results were found (Fig. S9). The effect of g_s formulation on

540   simulated photosynthesis was much smaller because of the lower sensitivity of the limiting rates of photosynthesis

541   to changes in c_i in the model compared to the effect of the same change in c_i on modelled g_s (Fig. S10 & S11).

542   Changes in g_s impact the partitioning of simulated energy fluxes. In general, increased g_s results in increased latent

543   heat and thus decreased sensible heat flux, and vice versa where g_s is decreased (Fig. S10 & S11). Also shown is

544   the effect of the MED model on O_3 flux into the leaf (Fig. S12 and Fig. S9 bottom panel). For the broadleaf tree

545   and C_3 herbaceous PFT, the MED model simulates a larger conductance and therefore a greater flux of O_3 through

546   stomata compared to JAC, and this is indicative of the potential for greater reductions in photosynthesis (Fig. S10

547   & S11 top row). The reverse is seen for the needle leaf tree, C_4 herbaceous and shrub PFTs.

548

549   Site level evaluation of the seasonal cycles of latent and sensible heat with both JAC and MED models compared

550   to FLUXNET observations showed in general, the MED model improved the seasonal cycle of both fluxes (lower

551   RMSE), but the magnitude of this varied from site to site (Fig. S13). At the deciduous broadleaf site, US-UMB,

552 MED resulted in improvements of the simulated seasonal cycle particularly in the summer months for both fluxes

553 (RMSE decreased from 42.7/31.5 to 38.5/28.0 W/m^2 for latent/sensible heat respectively). At the second

554 deciduous broadleaf site IT-CA1 however, there was almost no difference between the two g_s models. Both

555 evergreen needle leaf forest sites (FI-Hyy and DE-Tha) saw improvements in the simulated seasonal cycles of

556 latent and sensible heat with the MED model, primarily as a result of lower latent heat flux in the spring and

557 summer months, and higher sensible heat flux over the same period. At FI-Hyy, RMSE decreased from 10.1/7.4

558 to 6.7/6.7 W/m^2 for latent/sensible heat respectively, and at DE-Tha, RMSE decreased from 16.0/11.9 to 10.5/10.6

559 W/m^2 for latent/sensible heat respectively. With the MED model the monthly mean latent heat flux was improved

560 at the C$_3$ grass site (CH-Cha) as a result of increased flux in the summer months (RMSE decreased from 15.7 to

561 13.8 W/m^2), however there was no improvement in the sensible heat flux and RMSE with MED was increased

562 (from 3.9 to 4.9 W/m^2). At the C$_4$ grass site (US-SRG), small improvements were made in the seasonal cycle of

563 both latent and sensible heat with the MED model. At the deciduous savannah site (CG-Tch) which included a

564 high proportion of shrub PFT in the land cover type used in the site simulation, large improvements in the seasonal

565 cycle of both fluxes were simulated with the MED model, as a result of a decrease in the latent heat flux and an

566 increase in the sensible heat flux (RMSE decreased from 39.5/31.6 to 30.4/24.4 W/m^2 for latent/sensible heat

567 respectively).
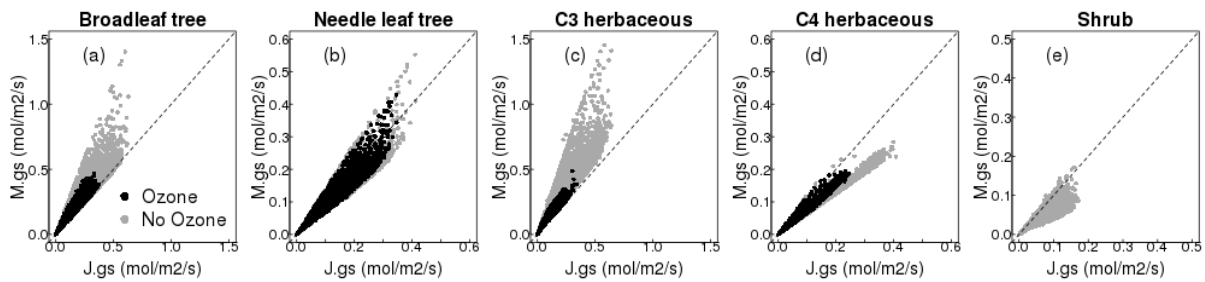
568

569 **Figure 2.** Comparison of simulated g_s with MED (y axis) versus JAC (x axis) for all five JULES PFTs at one grid

570 point (lat: 48.25; lon:, 5.25) shown are hourly values for the year 2000 (see SI section S3 for further details).

571

572 **3.2 Evaluation of the JULES O$_3$ model**

573 For all JULES scenarios similar spatial patterns of GPP are simulated compared to MTE (Fig. 3 and Fig. S14).

574 MTE estimates a mean GPP for present day in Europe of 938 gC m^2 yr^{-1} (Fig. 3). JULES tends to under-predict

575 GPP relative to the MTE product, estimates of GPP from JULES with both transient CO$_2$ and O$_3$

576 (run_both_CO2+O3) gives a mean across Europe of 813 gC m^2 yr^{-1} (high plant O$_3$ sensitivity) to 881 gC m^2 yr^{-1}

577 (low plant O$_3$ sensitivity), both of which are significantly different to the MTE product (t=27, $d.f.$=5750, p<2.2e$^-$

578 ^{16} (high); t=4.3, $d.f.$=5750, p<1.5e^{-05} (low); Fig. 3). Forcing with CO$_2$ alone (run_CO2) gives a mean GPP across

579 Europe of 900 to 923 gC m^2 yr^{-1} (high and low plant O$_3$ sensitivity respectively), and O$_3$ alone (run_O3 - without

580 the protective effect of CO$_2$) reduces estimated GPP to 732 to 799 gC m^2 yr^{-1} (Fig. S14). At latitudes >45°N JULES

581 has a tendency to under-predict MTE-GPP, and at latitudes <45 ^{o}N JULES tends to over-predict MTE-GPP (Fig.

582 S15). These regional differences are highlighted in Fig. S16, where in the Mediterranean region, JULES tends to

583 over-predict compared to MTE-GPP, so simulations with O$_3$ reduce the simulated GPP bringing it closer to MTE.

584 In the temperate region however, JULES tends to under-estimate MTE-GPP, so the addition of O_3 reduces
585 simulated GPP further (Fig. S16). In the boreal region, JULES under-predicts GPP, but to a lesser extent than in
586 the temperate region, and the addition of O_3 has less impact on reducing the GPP further (Fig. S16).

587
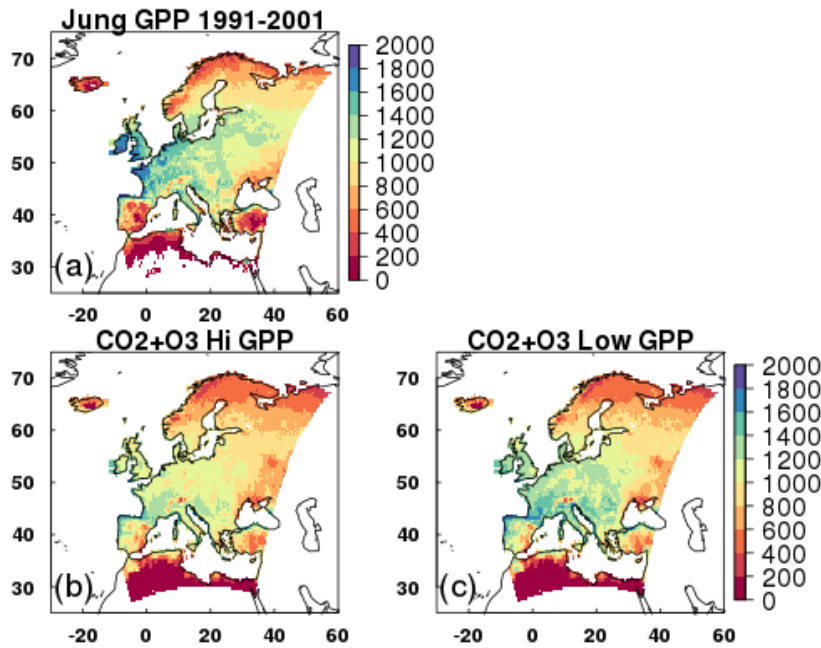
588

589 **Figure 3.** Mean GPP (g C m^2 yr^{-1}) from 1991 to 2001 for a) the observationally based globally extrapolated Flux
590 Network model tree ensemble (MTE) (Jung *et al*., 2011); b, c) model simulations with transient CO_2 and transient
591 O_3 (run_both_CO2+O3), high and low plant O_3 sensitivity respectively.

592

593

3.3 European simulations - Historical Period: 1901-2001

595

596 Over the historical period (1901-2001), run_O_3 reduced GPP under both the low and high plant O_3 sensitivity
597 parameterizations by -3% to -9% respectively (Table 1), and this difference in simulated GPP was significant
598 (t=102.2, *d.f.*=6270, p<2.2e^{-16}). Figure 4 highlights regional variations, however, where simulated reductions in
599 GPP are up to 20% across large areas of Europe, and up to 30% in some Mediterranean regions under the high
600 plant O_3 sensitivity. Some Boreal and Mediterranean regions show small increases in GPP over this period,
601 associated with O_3 induced stomatal closure enhancing water availability in these drier regions (Fig. 5). This
602 allows for greater stomatal conductance later in the year when soil moisture may otherwise have been limiting to
603 growth (up to 10%, Fig. 5), and therefore higher GPP, but these regions comprise only a small area of the entire
604 domain. Indeed, over much of the Europe, O_3-induced stomatal closure led to reduced g_s (up to 20%) across large
605 areas of temperate Europe and the Mediterranean, and even greater reductions in some smaller regions of southern
606 Mediterranean (Fig. 6), and these are not associated with notable increases in soil moisture availability (Fig. 5),
607 resulting in depressed GPP over much of Europe as described above. Under the low plant O_3 sensitivity, similar

spatial patterns occur, but the magnitude of GPP change (up to -10% across much of Europe) and g_s change (-5% to -10%) are lower compared to the high sensitivity. Over the twentieth century the land carbon sink is suppressed (-2% to -6%, Table 1). Large regional variation is shown in Figure 4, with temperate and Mediterranean Europe seeing a large reduction in land carbon storage, particularly under the high plant O_3 sensitivity (up to -15%).

Combined, the physiological response to changing CO_2 and O_3 concentrations (run_both_CO2+O3) results in a net loss of land carbon over the twentieth century under the high plant O_3 sensitivity (-2%, Table 1), dominated by loss of soil carbon (Table S3). This reflects the large increases in tropospheric O_3 concentration observed over this period (Fig. 1). Under the low plant O_3 sensitivity, the land carbon sink has started to recover by 2001 (+1.5%) owing to the recovery of the soil carbon pool beyond 1901 values over this period (Table S3).

To gain perspective on the magnitude of the O_3 induced flux of carbon from the land to the atmosphere we relate changes in total land carbon to carbon emissions from fossil fuel combustion and cement production for the EU-28-plus countries from the data of Boden et al. (2013). We recognise that our simulation domain is slightly larger than the EU28-plus as it includes a small area of western Russia so direct comparisons cannot be made, but this still provides a useful measure of the size of the carbon flux. For the period 1970 to 1979 the simulated loss of carbon from the European terrestrial biosphere due to O_3 effects on vegetation physiology was on average 1.32 Pg C (high vegetation sensitivity) and 0.71 Pg C (low vegetation sensitivity) (Table 2). This O_3 induced reduced C uptake of the land surface is equivalent to around 8% to 16% of the emissions of carbon from fossil fuel combustion and cement production over the same period for the EU28-plus countries (Table 2). Currently the emissions data availability goes up to 2011, over the last observable decade (2002 to 2011) the simulated reduction in land carbon due to O_3 has declined, but is still equivalent to 2% to 4% of the emissions of carbon from fossil fuels and cement production for the EU28-plus countries (Table 2). By comparison with one of the largest anthropogenic emissions of carbon for Europe, we show here the potential effect of O_3 on reducing the size of the European land carbon sink is notable.

3.4 European simulations - Future Period: 2001-2050

Over the 2001 to 2050 period, region-wide GPP with O_3 only changing (run_O3) increased marginally (+0.1% to +0.2%, high and low plant O_3 sensitivity, Table 1, with a significant difference between the two plant O_3 sensitivities (t=57, $d.f.$=6270 p<2.2e^{-16})), although with large spatial variability as discussed below (Fig. 4g & h). Figures S7 and S8 show that despite decreased tropospheric O_3 concentrations by 2050 in summer compared to 2001 levels, all regions are exposed to an increase in O_3 over the wintertime, and some regions of Europe, particularly temperate/Mediterranean experience increases in O_3 concentration in spring and autumn. Therefore, although in the O3 simulation, overall simulated GPP for Europe shows a small increase, large spatial variability is shown in Fig's 4g &h because of the variability in O_3 concentration with region and season. Increased GPP (dominantly 10%, but up to 20% in some areas) on 2001 levels is simulated across areas of Europe, however, decreases of up to 21% are simulated in some areas of the Mediterranean, up to 15% in some areas of the boreal region and up to 27% in the temperate zone (Fig. 4g & h).

When O_3 and CO_2 effects are combined (run_both_CO2+O3), simulated GPP increases (+15% to +18%, high/low plant O_3 sensitivities respectively, Table 1). This increase is greater than the enhancement simulated when CO_2 affects plant growth independently (run_CO2), because additional O_3 induced stomatal closure increases soil water availability in some regions, which enhances growth more in run_both_CO2+O3, compared to run_CO2. Nevertheless, although the percentage gain is larger, the absolute value of GPP by 2050 remains lower in run_both_CO2+O3 compared to GPP in run_CO2, highlighting the negative impact of O_3 at the land surface (Table S4).

Despite small increases in GPP in run_O3, the land carbon sink continues to decline from 2001 levels (-0.7% to -1.6%, low and high plant O_3 sensitivity respectively, Table 1). This is because the soil and vegetation carbon pools continue to lose carbon as they adjust slowly to small changes in input (GPP), i.e. the soil carbon pool is not in equilibrium in 2001, and is declining in response to reduced litter input as a result of 20th C O_3 impacts on GPP. Nevertheless, the negative effect of O_3 on the future land sink is markedly reduced relative to the historical period. Figure 4e & f however highlights regional differences. Boreal regions and parts of central Europe see minimal O_3 damage, whereas some areas of southern and northern Europe see further losses of up to 8% on 2001 levels. The run_both_CO2+O3 simulation is dominated by the physiological effects of changing CO_2, with land carbon sink increases of up to 7% (Table 1).

3.5 European simulations – Full experimental period: 1901-2050

From 1901 to 2050, run_O3 reduces GPP (-4% to -9%, with a significant difference between the low and high plant O_3 sensitivity (t=95, $d.f.$=6270 p<2.2e^{-16})) and land carbon storage (-3% to -7%, Table 1). Regionally, O_3 damage is lowest in the boreal zone, GPP decreases are largely between 5% to 8% / 2% to 4% for the high/low plant O_3 sensitivity respectively, with large areas minimally affected by O_3 damage (Figure 7), consistent with lower g_s of needle leaf trees that dominate this region, and so lower O_3 uptake (Fig. S17 & S18). In the temperate region, O_3 damage is extensive with reductions in GPP dominantly from 10% to 15% for the low and high plant O_3 sensitivity respectively. Across significant areas of this region reductions in GPP are up to 20% under high plant O_3 sensitivity (Figure 7). In the Mediterranean region, O_3 damage reduces GPP by 5% to 15% / 3% to 6% for the high/low plant O_3 sensitivity respectively, with some areas seeing greater losses of up to 20% under the high plant O_3 sensitivity, but this is less extensive than that seen in the temperate zone (Figure 7). In these drier regions, O_3 induced stomatal closure can increase available soil moisture (Fig. S17 & S18).

The run_both_CO2+O3 simulation shows that CO_2 induced stomatal closure can help alleviate O_3 damage by reducing the uptake of O_3 (Table S6). In these simulations, CO_2-induced stomatal closure was found to offset O_3-suppression of GPP, such that GPP by 2050 is 3% to 7% lower due to O_3 exposure (run_both_CO2+O3), rather than 4% to 9% lower in the absence of increasing CO_2 (run_O3, Table S6). Figure 6 shows this spatially, O_3 damage is reduced when the effect of atmospheric CO_2 on stomatal closure is accounted for, however despite this, the land carbon sink and GPP remain significantly reduced due to O_3 exposure.

687 From 1901 to 2050, run_both_CO2+O3 results in an increase in European land carbon uptake (+5% to +9%), and

688 an increase in GPP (+20% to +23%) by 2050 for the high and low plant O_3 sensitivity, respectively (Table 1).

689 Nevertheless, despite this increase there remains a large negative impact of O_3 on the European land carbon sink

690 (Fig. S19). By 2050 the simulated enhancement of land carbon and GPP in response to elevated CO_2 alone

691 (run_CO2) is reduced by 3% to 6% (land carbon) and 4% to 9% (GPP) for the low and high plant O_3 sensitivity

692 respectively, when O_3 is also accounted for (run_both_CO2+O3, Table 1). This is a large reduction in the ability

693 of the European terrestrial biosphere to sequester carbon.

694
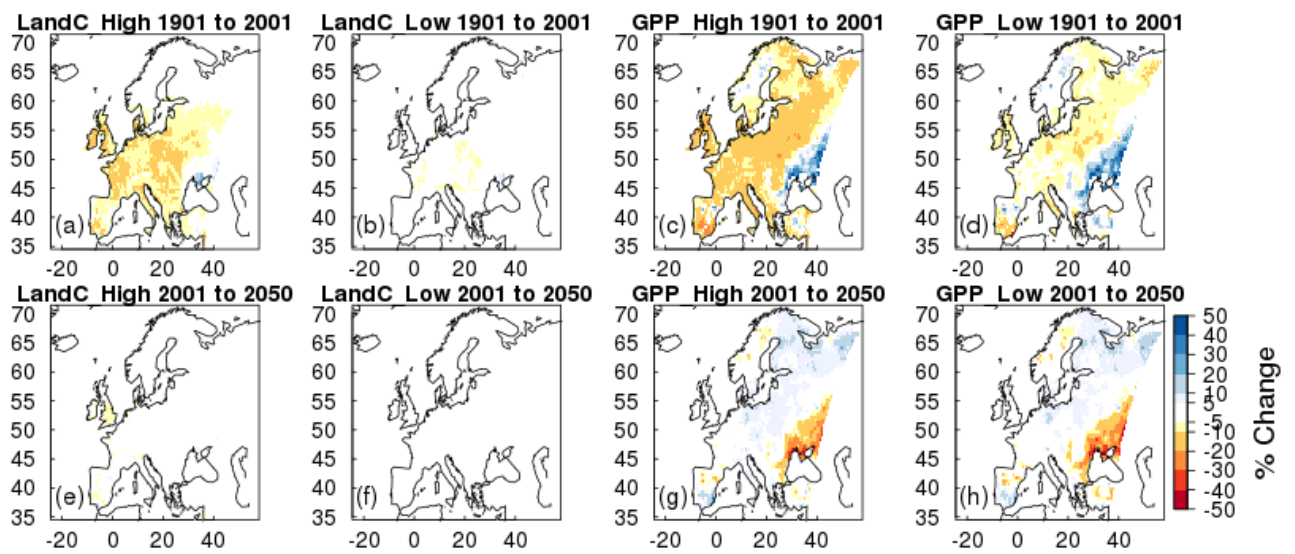
695

696 **Figure 4.** Simulated percentage change in total carbon stocks (Land C) and gross primary productivity (GPP) due

697 to O_3 effects at fixed pre-industrial atmospheric CO_2 concentration (run_O3). Changes are shown for the periods

698 1901 to 2001, and 2001 to 2050 for the high and low plant O_3 sensitivity.

699
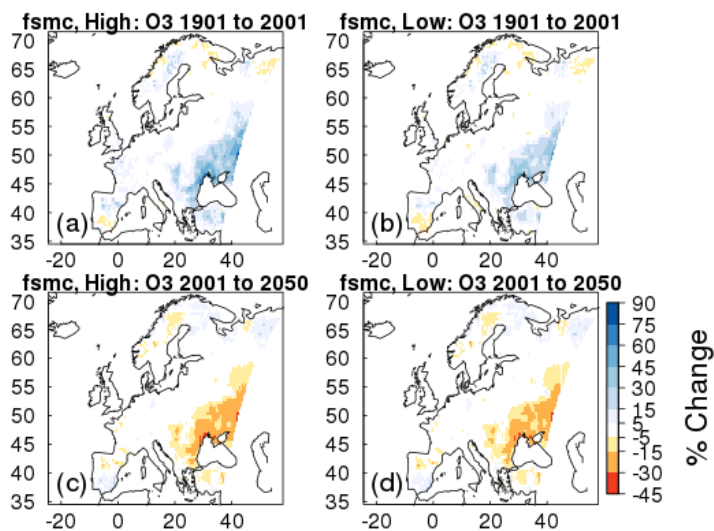
700

701   **Figure 5.** Simulated percentage change in plant available soil moisture (*fsmc*) due to O₃ effects at fixed pre-

702   industrial atmospheric CO_2 concentration (run_O3). Changes are shown for the periods 1901 to 2001, and 2001

703   to 2050 for the high and low plant O₃ sensitivity.

704
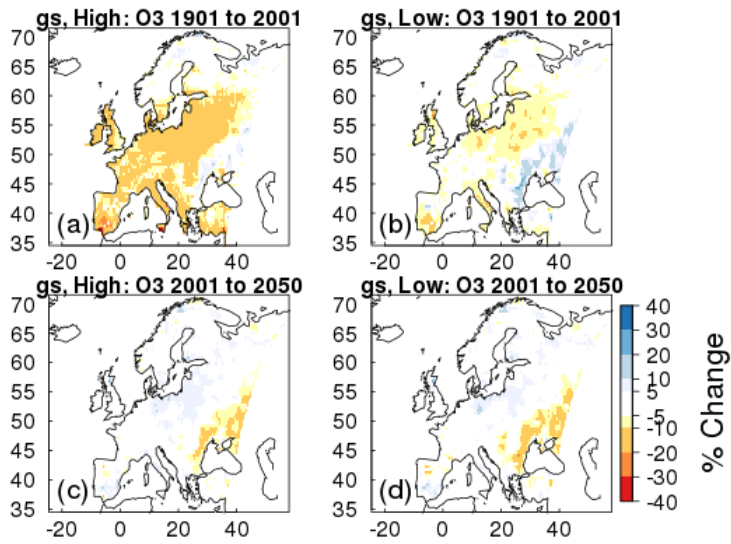
705

706   **Figure 6.** Simulated percentage change in stomatal conductance (g_s) due to O₃ effects at fixed pre-industrial

707   atmospheric CO_2 concentration (run_O3). Changes are shown for the periods 1901 to 2001, and 2001 to 2050 for

708   the high and low plant O₃ sensitivity.

709

710
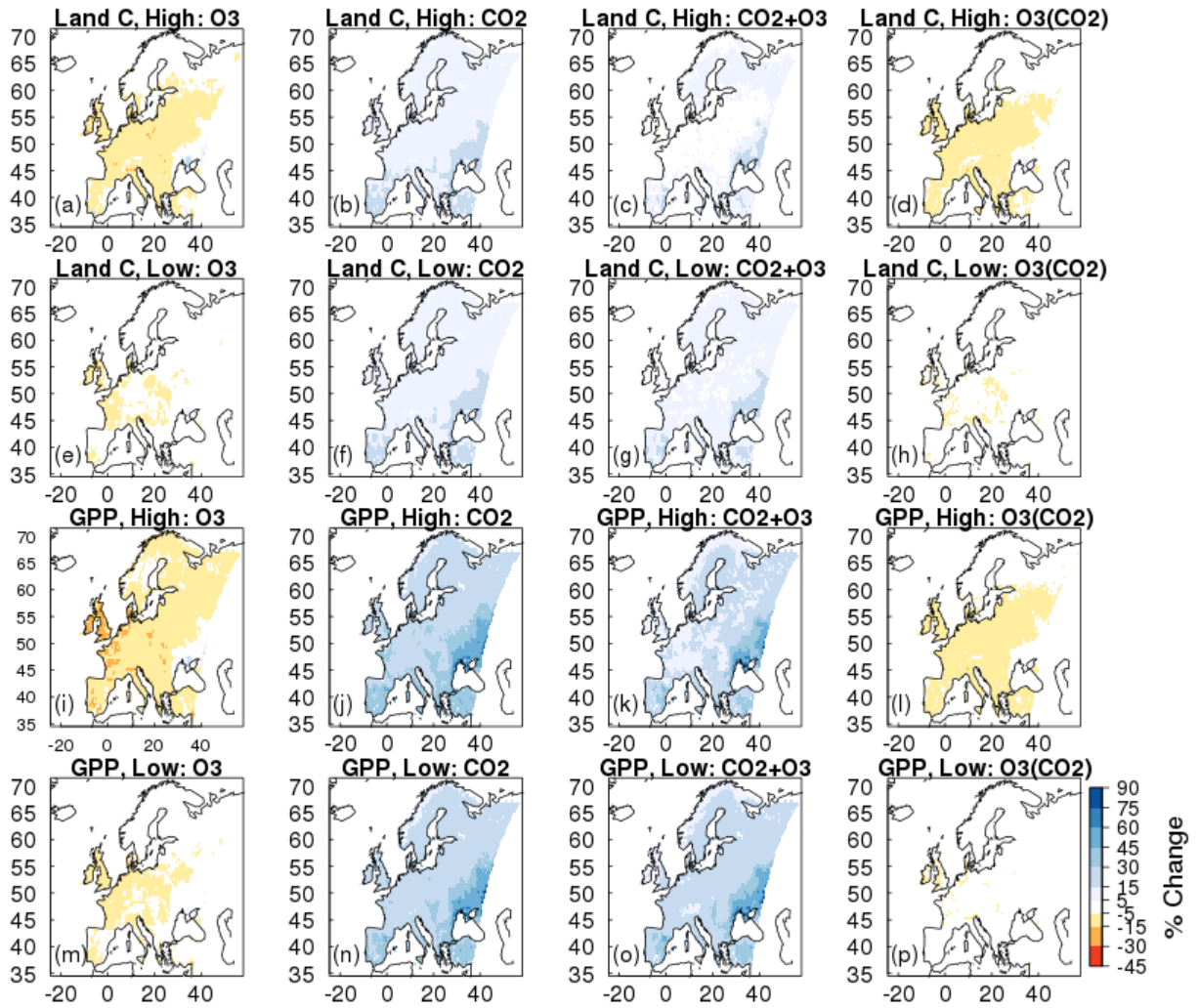
Figure 7. Simulated percentage change in total carbon stocks (Land C) and gross primary productivity (GPP) due to i) (a, e, i, m) O_3 effects at fixed pre-industrial atmospheric CO_2 concentration (run_O3), ii) (b, f, j, n) CO_2 fertilisation at fixed pre-industrial O_3 concentration (run_CO2), iii) (c, g, k, o) the interaction between O_3 and CO_2 effects (run_both_CO2+O3) iv) (d, h, l, p) O_3 effects with changing atmospheric CO_2 concentration (i.e. O_3 damage accounting for the effect of CO_2 induced stomatal closure; run_both_CO2+O3 – run_CO2). Changes are depicted for the periods 1901 to 2050 for high and lower ozone plant sensitivity.

	High Plant O₃ Sensitivity					
	1901 - 2001		**2001 - 2050**		**1901 - 2050**	
	GPP (Pg C yr⁻¹)	Land C (Pg C)	GPP (Pg C yr⁻¹)	Land C (Pg C)	GPP (Pg C yr⁻¹)	Land C (Pg C)
Value in 1901:	9.05	167	-	-	9.05	167
Absolute Change:						
O3	-0.81	-9.21	0.01	-2.44	-0.80	-11.65
CO2	1.16	4.24	1.42	12.98	2.58	17.22
CO2 + O3	0.13	-3.28	1.66	11.11	1.79	7.83
% Change:						
O3	-8.95	-5.51	0.12	-1.55	-8.84	-6.98
CO2	12.82	2.54	13.91	7.58	28.51	10.31
CO2 + O3	1.44	-1.96	18.08	6.79	19.78	4.69
	Low Plant O₃ Sensitivity					
	1901 - 2001		**2001 - 2050**		**1901 - 2050**	
	GPP (Pg C yr⁻¹)	Land C (Pg C)	GPP (Pg C yr⁻¹)	Land C (Pg C)	GPP (Pg C yr⁻¹)	Land C (Pg C)
Value in 1901:	9.34	167.5	-	-	9.34	167.5
Absolute Change:						
O3	-0.30	-3.59	0.02	-1.07	-0.40	-4.66
CO2	1.15	6.43	1.35	13.14	2.50	19.57
CO2 + O3	0.65	2.50	1.50	12.35	2.15	14.85
% Change:						
O3	-3.21	-2.14	0.22	-0.65	-4.28	-2.78
CO2	12.31	3.84	12.87	7.55	26.77	11.68
CO2 + O3	6.96	1.49	15.02	7.26	23.02	8.87

Table 1. Simulated changes in the European land carbon cycle due to changing O_3 and CO_2 concentrations (independently and together). Shown are changes in total carbon stocks (Land C) and gross primary productivity (GPP), over three different periods (historical: 1901 to 2001, future: 2001 to 2050, and full time series: 1901 to 2050). Absolute (top) and relative (bottom) differences are shown. For 2001 to 2050, please refer to Table S4 for the initial value for each run. See the SI for details of the estimation of the O_3 and CO_2 effects and their interaction.

	Mean (Pg C)				
	1970-1979	**1980-1989**	**1990-1999**	**2000-2009**	**2002-2011**
Modelled O$_3$ effect on land C sink :					
Higher sensitivity	-1.32	-1.01	-0.97	-0.53	-0.50
Low sensitivity	-0.71	-0.58	-0.50	-0.29	-0.26
Sum of C emissions from fossil fuel combustion and cement production (Pg C)	8.39	8.63	12.26	12.83	12.75
C lost from O$_3$ effect as a % of fossil fuel and cement emissions (%):					
Higher sensitivity	-15.73	-11.70	-7.91	-4.13	-3.92
Low sensitivity	-8.46	-6.72	-4.08	-2.26	-2.04

740

741 **Table 2.** Simulated change in total land carbon due to O$_3$ damage with changing atmospheric CO$_2$ concentration

742 for the two vegetation sensitivities. The sum of carbon emissions for each decade from fossil fuel combustion and

743 cement production for the EU-28 countries plus Albania, Bosnia and Herzegovina, Iceland, Belarus, Serbia,

744 Moldova, Norway, Turkey, Ukraine, Switzerland and Macedonia (EU28-plus) are shown, the data is from Boden

745 *et al.*, 2013. The simulated change in land carbon as a result of O$_3$ damage is depicted as a percentage of the EU28-

746 plus emissions to demonstrate the magnitude of the additional source of carbon to the atmosphere from plant O$_3$

747 damage.

748

749 **4 Discussion**

750

751 **4.1 Evaluation of g_s models and JULES O$_3$ model**

752

753 Comparison of the new g_s model implemented in this study (MED) with the g_s model currently used as standard

754 in JULES (JAC) revealed large differences in g_s for each PFT, principally as a result of the data-based

755 parameterisation of the new model. Water use increased for the broadleaf tree and C$_3$ herbaceous PFTs using the

756 MED model compared to JAC, but decreased for the needle leaf tree, C$_4$ herbaceous and shrub PFTs which

757 displayed a more conservative water use strategy compared to JAC. These changes are in line with the work of

758 De Kauwe et al. (2015) who found a reduction in annual transpiration for evergreen needle leaf, tundra and C$_4$

759 grass regions when implementing the Medlyn g_s model into the Australian land surface scheme CABLE. Site-

760 level evaluation of the models against Fluxnet observations showed that in general the MED model improved

761 simulated seasonal cycles of latent and sensible heat. The magnitude of the improvement varied with site,

762 improvements were seen at the deciduous savanna site, and at the NT sites and BT site (US_UMB) in the spring

763 and summer. However, much smaller improvements were seen at the grass sites. Changes in g_s in this study

764 resulted in differences in latent and sensible heat fluxes. Changes in the partitioning of energy fluxes at the land

765 surface could have consequences for the intensity of heatwaves (Cruz et al., 2010;Kala et al., 2016), runoff (Betts

766 et al., 2007;Gedney et al., 2006) and rainfall patterns (de Arellano et al., 2012), although fully coupled simulations

767 would be necessary to detect these effects. The differences in simulated g_s led to differences in uptake of O$_3$

768 between the two models because the rate of g_s is the predominant determinant of the flux of O$_3$ through stomata.

769   Higher O_3 uptake is indicative of greater damage. Therefore, given that C_3 herbaceous vegetation is the dominant

770   land cover class across the European domain used in this study, this suggests a greater O_3 impact for Europe would

771   be simulated with MED model compared to JAC in our simulations where chemistry is uncoupled from the land

772   surface.

773

774   We evaluated the JULES O_3 model by comparing modelled GPP against the Jung et al (2011) MTE product.

775   Similar spatial patterns of GPP were simulated by JULES compared to MTE. Zonal means also showed similar

776   patterns of GPP, although JULES under predicted GPP compared to MTE at latitudes >45ºN (temperate and boreal

777   regions; all simulations) and over predicted GPP at latitudes <45ºN (Mediterranean region; all simulations). The

778   simulations with transient O_3 (i.e. O3 and CO2+O3) showed large differences in GPP between the high and low

779   plant O_3 sensitivity simulations, this is to be expected given that the high plant O_3 sensitivity simulations were

780   parameterised to be 'damaged' more by O_3, i.e. greater reduction of photosynthesis/g_s with O_3 exposure compared

781   to the low plant O_3 sensitivity simulations. This difference was largest in the temperate zone, largely because of

782   C_3 grass cover being the dominant land cover here and the difference in the sensitivity to O_3 between the high and

783   low calibrations is significantly larger for C_3 grasses compared to the needle leaf trees that dominate in the boreal

784   region. Additionally, a longer growing season in the temperate region may allow for greater uptake of O_3 into

785   vegetation. C_3 grass is also the dominant land cover in the Mediterranean region with a different calibration used

786   for Mediterranean grasses for the low plant O_3 sensitivity which is less sensitive to O_3 than the temperate C_3

787   grasses, but high soil moisture stress is common throughout the growing season in the Mediterranean limiting the

788   uptake of O_3 through stomata, which likely diminishes the difference between the high and low calibrations. In

789   general, incorporating plant O_3 damage into JULES leads to worse agreement with the MTE GPP product,

790   however, this is expected to some degree as we are adding an explicit representation of O_3 damage to a model

791   calibrated to reproduce current day GPP and draw down of atmospheric CO_2. Inevitably this implicitly includes

792   O_3 damage to vegetation. Explicit representation of plant O_3 damage is important to investigate how O_3 damage

793   changes through time, under different emissions scenario's, and the interactive effects with other gases (such as

794   CO_2) and with climate change. The percentage changes we simulate are therefore important to demonstrate the

795   sensitivity of modelled GPP and land Carbon to this process.

796

797   **4.2 Comparison of modelled estimates of O_3 damage**

798

799   Our estimates suggest O_3 (run_O3) reduced GPP by 2001 by 3% to 9% on average across Europe and NPP by 5%

800   to 11% for the low and high plant O_3 sensitivities respectively (Table S3). Anav et al. (2011) simulated a 22%

801   reduction of GPP across Europe for 2002 using the ORCHIDEE model. Present day O_3 exposure reduced GPP by

802   10% to 25% in Europe, and 10.8% globally in the study by Lombardozzi et al. (2015) using the Community land

803   model (CLM). O_3 reduced NPP by 11.2% in Europe from 1989 to 1995 using the Terrestrial Ecosystem Model

804   (TEM) (Felzer et al., 2005). Globally, concentrations of O_3 predicted for 2100 reduced GPP by 14% to 23% using

805   a former parameterisation of O_3 sensitivity in JULES (Sitch et al., 2007). The recent study by Franz et al. (2017)

806   showed mean GPP declined by 4.7% over the period 2001 to 2010 using the OCN model over the same European

807   domain and using the same O_3 forcing produced by EMEP MSC-W as used in this study. Our estimates of changes

808   in current day GPP and NPP are at the lower end of previously modelled estimates. Simulated O_3 impacts will be

809   dependent on model O_3 concentrations, meteorology, plant sensitivity to O_3, and process representation of O_3

810   damage. It is therefore difficult to hypothesise as to exactly why modelled estimates differ, but suggests that an

811   ensemble approach to modelling O_3 impacts on the terrestrial biosphere would be beneficial to understand some

812   of these differences and provide estimates of O_3 damage with uncertainties.

813

814   **4.3 Impacts of O_3 at the land surface**

815

816   In this study, O_3 has a detrimental effect on the size of the land carbon sink for Europe. This is primarily through

817   a decrease in the size of the soil carbon pool as a result of reduced litter input to the soil, consistent with reduced

818   GPP/NPP. Field studies show that in some regions of Europe, soil carbon stocks are decreasing (Bellamy et al.,

819   2005;Capriel, 2013;Heikkinen et al., 2013;Sleutel et al., 2003). The study of Bellamy et al. (2005), for example,

820   showed that carbon was lost from soils across England and Wales between 1978 to 2003 at a mean rate of 0.6%

821   per year with little effect of land use on the rate of carbon loss, suggesting a possible link to climate change. It is

822   understood that climate change is likely to affect soil carbon turnover. Increased temperatures increase microbial

823   decomposition activity in the soil, and therefore increase carbon losses through higher rates of respiration (Cox et

824   al., 2000;Friedlingstein et al., 2006;Jones et al., 2003). However, some studies have found that O_3 can decrease

825   soil carbon content. Talhelm et al. (2014), for example, found O_3 reduced carbon content in near surface mineral

826   soil of forest soils exposed to 11 years of O_3 fumigation. Hofmockel et al. (2011) found elevated O_3 reduced the

827   carbon content in more stable soil organic matter pools, and Loya et al. (2003) showed that the fraction of soil

828   carbon formed in forest soils over a 4 year experimental period when fumigated with both CO_2 and O_3 was reduced

829   by 51% compared to the soil fumigated with CO_2 alone. It is agreed that amongst other factors that change with

830   O_3 exposure such as litter quality and composition, reduced litter quantity also has significant detrimental

831   consequences for soil carbon stocks (Andersen, 2003;Lindroth, 2010;Loya et al., 2003). Results from this study

832   therefore suggest that increasing tropospheric O_3 may be a contributing factor to the declining soil carbon stocks

833   observed across Europe as a result of reduced litter input to the soil carbon pool consistent with reduced NPP.

834

835   We acknowledge, however, that our model simulations do not include coupling of Nitrogen and Carbon cycles,

836   or land management practices. We include a representation of agricultural regions through the model calibration

837   against the wheat O_3 sensitivity function (CLRTAP, 2017), and in our simulations the high plant O_3 sensitivity

838   scenario uses this calibration against wheat for all C_3/C_4 land cover which dominates our model domain. Wheat is

839   known to be one of the most O_3 sensitive crop species however, so it is possible that our simulations over-estimate

840   the O_3 impact at the land surface. However, the low plant O_3 sensitivity calibration against natural grasslands

841   provides a counter estimate of the impact of O_3 at the land surface, therefore it is important to consider the range

842   our results provide (i.e. both the high and low plant O_3 sensitivity) as an indicator of the impact of O_3 on the land

843   surface. As with all uncoupled modelling studies, a change in g_s and flux will impact the O_3 concentration itself.

844   Therefore adopting the Medlyn formulation with a higher g_s and subsequently higher O_3 flux for broadleaf and C_3

845   PFTs (Fig 2) would lead to reduced O_3 concentration, which in turn maydampen the effect of higher g_s on O_3 flux,

846   although the higher uptake of O_3 by vegetation may lead to more damage and increase O_3 concentrations, in an

847 uncoupled chemistry-land modelling system such as this it is not possible to predict which process would
848 dominate. Additionally, this version of JULES does not have a crop module; it has no land management practices
849 such as harvesting, ploughing or crop rotation – processes which may have counteracting effects on the land
850 carbon sink. Further, without a coupled Carbon and Nitrogen cycle, it is likely that the CO_2 fertilisation response
851 of GPP and the land carbon sink is over estimated in some regions of our simulations since nitrogen availability
852 limits terrestrial carbon sequestration of natural ecosystems in the temperate and boreal zone (Zaehle, 2013). This
853 would have consequences for our modelled O_3 impact, particularly into the future where the large CO_2 fertilisation
854 effect was responsible for partly offsetting the negative impact of O_3. Although in our simulations a high fraction
855 of land cover is agricultural which we assume would be optimally fertilised. Our simulations also use a fixed
856 climate, so we do not include the effect of climate change on shifting plant phenology. Therefore, our results may
857 underestimate plant O_3 damage, since if the growing season started earlier or finished later, plants in some regions
858 would be exposed to higher O_3 concentrations. Nevertheless, we emphasise that this study provides a sensitivity
859 assessment of the impact of plant O_3 damage on GPP and the land carbon sink.

860

861 Another caveat we fully acknowledge is that at the leaf-level JULES is parameterised to reduce g_s with O_3
862 exposure. Whilst this response is commonly observed (Wittig et al., 2007;Ainsworth et al., 2012), there is evidence
863 to suggest that O_3 impairs stomata in some species, making them non-responsive to environmental stimuli (Hayes
864 et al., 2012;Hoshika et al., 2012a;Mills et al., 2009;Paoletti and Grulke, 2010). In drought conditions the
865 mechanism is thought to involve O_3 stimulated ethylene production which interferes with the stomatal response
866 to ABA signalling (Wilkinson and Davies, 2009;Wilkinson and Davies, 2010). Such stomatal sluggishness can
867 result in higher O_3 uptake and injury, increased water-loss, and therefore greater vulnerability to environmental
868 stresses (Mills et al., 2016). McLaughlin (2007a;2007b) and Sun et al. (2012) provide evidence of increased
869 transpiration and reduced streamflow in forests at the regional scale in response to ambient levels of O_3, and
870 suggest this could increase the frequency and severity of droughts. Hoshika et al. (2012b) however found that
871 despite sluggish stomatal control in O_3 exposed trees, whole tree water use was lower in these trees because of
872 lower gas exchange and premature leaf shedding of injured leaves. To our knowledge, the study of Hoshika et al.
873 (2015) is the first to include an explicit representation of sluggish stomatal control in a land-atmosphere model,
874 they show that sluggish stomatal behaviour has implications for carbon and water cycling in ecosystems.
875 However, it is by no means a ubiquitous response, and it is not fully understood which species respond this way
876 and under what conditions (Mills et al., 2016;Wittig et al., 2007). Nevertheless, this remains an important area of
877 future work.

878

879 In this work we implement the stomatal closure proposed in Medlyn et al., (2011), this uses the parameter g_l.
880 Hoshika et al. (2013) show a significant difference in the g_l parameter (higher in elevated O_3 compared to ambient)
881 in Siebold's beech in June of their experiment. However, this is only at the start of the growing season, further
882 measurements show no difference in this parameter between O_3 treatments. Quantifying an O_3 effect directly on
883 g_l would require a detailed meta-analysis of empirical data on photosynthesis and g_s for different PFTs, which is
884 currently lacking in the literature.

885

886

887   A further caveat of this study is that the O_3 concentrations used to force the model are offline, in this case generated

888   by the EMEP MSC-W model. This means the depositional sink is different in JULES (Medlyn formulation),

889   compared to the EMEP model which uses the g_s formulation presented in Emberson et al. (2000) and Emberson

890   et al. (2001). Because we link two different model systems, the g_s values in the EMEP model differ from those

891   obtained using the Medlyn formulation, which would ultimately lead to different O_3 concentrations. The role of

892   EMEP in this study is to provide O_3 concentrations at the top of the vegetation canopy to force JULES and not g_s,

893   how the different depositional sinks would affect simulated O_3 concentrations at canopy height has not been

894   investigated.

895

896   These offline simulations show the sensitivity of GPP and the land carbon sink to tropospheric O_3, suggesting that

897   O_3 is an important predictor of future GPP and the land carbon store across Europe. There are uncertainties in our

898   estimates however from the use of uncoupled tropospheric chemistry, meteorology and stomatal function. For

899   example, increased frequency of drought in the future would reduce stomatal conductance (assuming no sluggish

900   stomatal response) and thus O_3 uptake. Since our offline simulations do not include this feedback it is possible the

901   O_3 effect is over estimated here. Given the complexity of potential interactions and feedbacks it remains difficult

902   to diagnose the importance of individual factors (e.g. the direct physiological response) in a fully coupled

903   simulation. Once the importance of a process is demonstrated offline, it provides evidence of the need to

904   incorporate such process in coupled regional and global simulations.

905

906   **4.4 O_3 as a missing component of carbon cycle assessments?**

907

908   Comprehensive analyses of the European carbon balance suggest a large biogenic carbon sink (Janssens et al.,

909   2003;Luyssaert et al., 2012;Schulze et al., 2009). However, estimates are hampered by large uncertainties in key

910   components of the land carbon balance, such as estimates of soil carbon gains and losses (Ciais et al.,

911   2010;Janssens et al., 2003;Schulze et al., 2009;Schulze et al., 2010). We suggest that the effect of O_3 on plant

912   physiology is a contributing factor to the decline in soil carbon stores observed across Europe, and as such this O_3

913   effect is a missing component of European carbon cycle assessments. Over the full experimental period (1901 to

914   2050), our results show elevated O_3 concentrations reduce the amount of carbon that can be stored in the soil by

915   3% to 9% (low and high plant O_3 sensitivity, respectively), which almost completely offsets the beneficial effects

916   of CO_2 fertilisation on soil carbon storage under the high plant O_3 sensitivity . This would contribute to a change

917   in the size of a key carbon sink for Europe, and is particularly important when we consider the evolution of the

918   land carbon sink into the future given the impact of O_3 on soil carbon sequestration and the high uncertainty of

919   future tropospheric O_3 concentrations. Schulze et al. (2009) and Luyssaert et al. (2012) extended their analysis of

920   the European carbon balance to include additional non-CO_2 greenhouse gases (CH_4 and N_2O). Both studies found

921   that emissions of these offset the biogenic carbon sink, reducing the climate mitigation potential of European

922   ecosystems. This highlights the importance of accounting for all fluxes and stores in carbon/greenhouse gas

923   balance assessments, of which O_3 and its indirect effect on the CO_2 flux via direct effects on plant physiology is

924   currently missing.

925

926   **4.5 Interactive effects of O_3 and CO_2**

928   We looked at the interactive effects of CO_2 and O_3. Our results support the hypothesis that elevated atmospheric

929   CO_2 provides some protection against O_3 damage because of lower g_s that reduces uptake of O_3 through stomata

930   (Harmens et al., 2007;Wittig et al., 2007). In the present study, reductions in GPP and the land carbon store due

931   to O_3 exposure were lower when simulated with concurrent changes in atmospheric CO_2. Despite acclimation of

932   photosynthesis after long-term exposure to elevated atmospheric CO_2 of field grown plants (Ainsworth and Long,

933   2005;Medlyn et al., 1999), there is no evidence to suggest that g_s acclimates (Ainsworth et al., 2003;Medlyn et al.,

934   2001). This suggests the protective effect of elevated atmospheric CO_2 against O_3 damage will be sustained in the

935   long term. However, although meta-analysis suggest a general trend of reduced g_s with elevated CO_2 (Ainsworth

936   and Long, 2005;Medlyn et al., 1999), this is not a universal response. Stomatal responses on exposure to elevated

937   CO_2 with FACE treatment varied with genotype and growth stage in a fast-growing poplar community (Bernacchi

938   et al., 2003;Tricker et al., 2009). In other mature forest stands, limited stomatal response to elevated CO_2 was

939   observed after canopy closure (Ellsworth, 1999;Uddling et al., 2009). Also, some studies found that stomatal

940   responses to CO_2 were significant only under high atmospheric humidity (Cech et al., 2003;Leuzinger and Körner,

941   2007;Wullschleger et al., 2002). These examples illustrate that stomatal responses to elevated atmospheric CO_2

942   are not universal, and as such the protective effect of CO_2 against O_3 injury cannot be assumed for all species, at

943   all growth stages under wide ranging environmental conditions.

944

945   **5 Conclusion**

946

947   What is abundantly clear is that plant responses to both CO_2 and O_3 are complicated by a host of factors that are

948   only partly understood, and it remains difficult to identify general, global patterns given that effects of both gases

949   on plant communities and ecological interactions are highly context and species specific (Ainsworth and Long,

950   2005;Fuhrer et al., 2016;Matyssek et al., 2010b). This study quantifies the sensitivity of the land carbon sink for

951   Europe and GPP to changing concentrations of atmospheric CO_2 and O_3 from 1901 to 2050. We have used a state

952   of the art land surface model calibrated for European vegetation to give our best estimates of this sensitivity within

953   the limits of data availability to calibrate the model for O_3 sensitivity, current knowledge and model structure. In

954   summary, this study has shown that potential gains in terrestrial carbon sequestration over Europe resulting from

955   elevated CO_2 can be partially offset by concurrent rises in tropospheric O_3 over 1901-2050. Specifically, we have

956   shown that the negative effect of O_3 on the land carbon sink was greatest over the twentieth century, when O_3

957   concentrations increased rapidly from pre-industrial levels. Over this period soil carbon stocks were diminished

958   over agricultural areas, consistent with reduced NPP and litter input. This loss of soil carbon was largely

959   responsible for the decrease in the size of the land carbon sink over Europe. The O_3 effect on the land carbon store

960   and flux was reduced into the future as CO_2 concentration rose considerably and changes in O_3 concentration were

961   less pronounced. However, there remained a large cumulative negative impact on the land carbon sink for Europe

962   by 2050. The interaction between the two gases was found to reduce O_3 injury owing to reduced stomatal opening

963   in elevated atmospheric CO_2. However, primary productivity and land carbon storage remained suppressed by

964   2050 due to plant O_3 damage. Expressed as a percentage of the emissions from fossil fuel and cement production

965   for the EU28-plus countries, the carbon emissions from O_3-induced plant injury are a source of anthropogenic

966   carbon previously not accounted for in carbon cycle assessments. Our results demonstrate the sensitivity of

967 modelled terrestrial carbon dynamics to the direct effect of tropospheric O_3 and its interaction with atmospheric
968 CO_2 on plant physiology, demonstrating this process is an important predictor of future GPP and trends in the
969 land-carbon sink. Nevertheless, this process remains largely unconsidered in regional and global climate model
970 simulations that are used to model carbon sources and sinks and carbon-climate feedbacks.

971
972
973

974 **Data availability**

975

976 The JULES model can be downloaded from the Met Office Science Repository Service
977 (https://code.metoffice.gov.uk/trac/jules - see here for a helpful how to http://jules.jchmr.org/content/getting-
978 started). Model output data presented in this paper and the exact version of JULES with namelists are available
979 upon request from the corresponding author.

980

981 **Supplementary Information**

982

983 Supplementary_Information_Oliver_et_al_vn4.0.docx

984

985 **Competing Interests**
986 The authors declare that they have no conflict of interest

987

988 **Acknowledgements**

989

990 RJO and LMM were supported by the EU FP7 (ECLAIRE, 282910) and JWCRP (UKESM, NEC05816). This
991 work was also supported by EMEP under UNECE. SS and LMM acknowledge the support of the NERC
992 SAMBBA project (NE/J010057/1). The UK Met Office contribution was funded by BEIS under the Hadley Centre
993 Climate Programme (GA01101). GAF also acknowledges funding from the EU's Horizon 2020 research and
994 innovation programme (CRESCENDO, 641816). We also thank Magnuz Engardt of SMHI for providing the
995 RCA3 climate dataset. This work used eddy covariance data acquired and shared by the FLUXNET community,
996 including these networks: AmeriFlux, AfriFlux, AsiaFlux, CarboAfrica, CarboEuropeIP, CarboItaly, CarboMont,
997 ChinaFlux, Fluxnet-Canada, GreenGrass, ICOS, KoFlux, LBA, NECC, OzFlux-TERN, TCOS-Siberia, and
998 USCCC. The ERA-Interim reanalysis data are provided by ECMWF and processed by LSCE. The FLUXNET
999 eddy covariance data processing and harmonization was carried out by the European Fluxes Database Cluster,
1000 AmeriFlux Management Project, and Fluxdata project of FLUXNET, with the support of CDIAC and ICOS
1001 Ecosystem Thematic Center, and the OzFlux, ChinaFlux and AsiaFlux offices. We also thank the two anonymous
1002 reviewers who helped to improve this manuscript.

1003
1004
1005 **References**

1006

1007 Ainsworth, E., and Long, S.: What have we learned from 15 years of free-air CO_2 enrichment (FACE)?
1008 A meta-analytic review of the responses of photosynthesis, canopy properties and plant production
1009 to rising CO2, New Phytologist, 165, 351-372, 2005.
1010 Ainsworth, E. A., Davey, P. A., Hymus, G. J., Osborne, C. P., Rogers, A., Blum, H., Nosberger, J., and
1011 Long, S. P.: Is stimulation of leaf photosynthesis by elevated carbon dioxide concentration
1012 maintained in the long term? A test with *Lolium perenne* grown for 10 years at two nitrogen
1013 fertilization levels under Free Air CO_2 Enrichment (FACE), Plant, Cell and Environment, 26, 705-714,
1014 2003.
1015 Ainsworth, E. A.: Rice production in a changing climate: a meta-analysis of responses to elevated
1016 carbon dioxide and elevated ozone concentration, Global Change Biology, 14, 1642-1650,
1017 10.1111/j.1365-2486.2008.01594.x, 2008.
1018 Ainsworth, E. A., Yendrek, C. R., Sitch, S., Collins, W. J., and Emberson, L. D.: The Effects of
1019 Tropospheric Ozone on Net Primary Productivity and Implications for Climate Change, Annual
1020 Review of Plant Biology, 63, 637-661, doi:10.1146/annurev-arplant-042110-103829, 2012.
1021 Anav, A., Menut, L., Khvorostyanov, D., and Viovy, N.: Impact of tropospheric ozone on the Euro-
1022 Mediterranean vegetation, Global change biology, 17, 2342-2359, 2011.
1023 Andersen, C. P.: Source–sink balance and carbon allocation below ground in plants exposed to
1024 ozone, New Phytologist, 157, 213-228, 10.1046/j.1469-8137.2003.00674.x, 2003.
1025 Arneth, A., Harrison, S. P., Zaehle, S., Tsigaridis, K., Menon, S., Bartlein, P. J., Feichter, J., Korhola, A.,
1026 Kulmala, M., O'Donnell, D., Schurgers, G., Sorvari, S., and Vesala, T.: Terrestrial biogeochemical
1027 feedbacks in the climate system, Nature Geosci, 3, 525-532,
1028 http://www.nature.com/ngeo/journal/v3/n8/suppinfo/ngeo905_S1.html, 2010.
1029 Auvray, M., and Bey, I.: Long-range transport to Europe: Seasonal variations and implications for the
1030 European ozone budget, Journal of Geophysical Research: Atmospheres, 110,
1031 doi:10.1029/2004JD005503, 2005.
1032 Avnery, S., Mauzerall, D. L., Liu, J., and Horowitz, L. W.: Global crop yield reductions due to surface
1033 ozone exposure: 1. Year 2000 crop production losses and economic damage, Atmospheric
1034 Environment, 45, 2284-2296, https://doi.org/10.1016/j.atmosenv.2010.11.045, 2011.
1035 Baig, S., Medlyn, B. E., Mercado, L. M., and Zaehle, S.: Does the growth response of woody plants to
1036 elevated CO2 increase with temperature? A model-oriented meta-analysis, Global Change Biology,
1037 21, 4303-4319, 10.1111/gcb.12962, 2015.
1038 Bellamy, P. H., Loveland, P. J., Bradley, R. I., Lark, R. M., and Kirk, G. J.: Carbon losses from all soils
1039 across England and Wales 1978–2003, Nature, 437, 245-248, 2005.
1040 Bernacchi, C. J., Calfapietra, C., Davey, P. A., Wittig, V. E., Scarascia-Mugnozza, G. E., Raines, C. A.,
1041 and Long, S. P.: Photosynthesis and stomatal conductance responses of poplars to free-air CO_2
1042 enrichment (PopFACE) during the first growth cycle and immediately following coppice., New
1043 Phytologist, 159, 609-621, 2003.
1044 Best, M. J., Pryor, M., Clark, D. B., Rooney, G. G., Essery, R. L. H., Menard, C. B., Edwards, J. M.,
1045 Hendry, M. A., Porson, N., Gedney, N., Mercado, L. M., Sitch, S., Blyth, E., Boucher, O., Cox, P. M.,
1046 Grimmond, C. S. B., and Harding, R. J.: The Joint UK Land Environment Simulator (JULES), Model
1047 description - Part 1: Energy and water fluxes, Geoscientific Model Development Discussions, 4, 595-
1048 640, 10.5194/GMDD-4-595-2011, 2011.
1049 Betts, R. A., Boucher, O., Collins, M., Cox, P. M., Falloon, P. D., Gedney, N., Hemming, D. L.,
1050 Huntingford, C., Jones, C. D., and Sexton, D. M.: Projected increase in continental runoff due to plant
1051 responses to increasing carbon dioxide, Nature, 448, 1037-1041, 2007.
1052 Boden, T. A., Marland, G., and Andres, R. J.: Global, Regional, and National Fossil-Fuel CO2 Emissions,
1053 Oak Ridge National Laboratory, U.S. Department of Energy, Oak Ridge, Tenn., USA, 2013.
1054 Büker, P., Feng, Z., Uddling, J., Briolat, A., Alonso, R., Braun, S., Elvira, S., Gerosa, G., Karlsson, P. E.,
1055 Le Thiec, D., Marzuoli, R., Mills, G., Oksanen, E., Wieser, G., Wilkinson, M., and Emberson, L. D.: New

flux based dose-response relationships for ozone for European forest tree species, Environmental Pollution, 163-174, 2015.

Calvete-Sogo, H., Elvira, S., Sanz, J., González-Fernández, I., García-Gómez, H., Sánchez-Martín, L., Alonso, R., and Bermejo-Bermejo, V.: Current ozone levels threaten gross primary production and yield of Mediterranean annual pastures and nitrogen modulates the response, Atmospheric Environment, 95, 197-206, http://dx.doi.org/10.1016/j.atmosenv.2014.05.073, 2014.

Capriel, P.: Trends in organic carbon and nitrogen contents in agricultural soils in Bavaria (south Germany) between 1986 and 2007, European Journal of Soil Science, 64, 445-454, 2013.

Cech, P. G., Pepin, S., and Korner, C.: Elevated CO_2 reduces sap flux in mature deciduous forest trees, Oecologia, 137, 258-268, 2003.

Ceulemans, R., and Mousseau, M.: Effects of elevated atmospheric CO_2 on woody plants, New Phytologist, 127, 1994.

Ciais, P., Wattenbach, M., Vuichard, N., Smith, P., Piao, S., Don, A., Luyssaert, S., Janssens, I., Bondeau, A., and Dechow, R.: The European carbon balance. Part 2: croplands, Global Change Biology, 16, 1409-1428, 2010.

Ciais, P., Sabine, C., Bala, G., Bopp, L., Brovkin, V., Canadell, J., Chhabra, A., DeFries, R., Galloway, J., Heimann, M., Jones, C., Le Quéré, C., Myneni, R. B., Piao, S., and Thornton, P.: Carbon and Other Biogeochemical Cycles. In: Climate Change 2013: The Physical Science Basis. Contribution of Working Group I to the Fifth Assessment Report of the Intergovernmental Panel on Climate Change [Stocker, T.F., D. Qin, G.-K. Plattner, M. Tignor, S.K. Allen, J. Boschung, A. Nauels, Y. Xia, V. Bex and P.M. Midgley (eds.)]. Cambridge University Press, Cambridge, United Kingdom and New York, NY, USA., 2013.

Clark, D. B., Mercado, L. M., Sitch, S., Jones, C. D., Gedney, N., Best, M. J., Pryor, M., Rooney, G. G., Essery, R. L. H., Blyth, E., Boucher, O., Harding, R. J., and Cox, P. M.: The Joint UK Land Environment Simulator (JULES), Model description - Part 2: Carbon fluxes and vegetation, Geoscientific Model Development Discussions, 4, 641-688, 10.5194/gmdd-4-641-2011, 2011.

CLRTAP: The UNECE Convention on Long-range Transboundary Air Pollution. Manual on Methodologies and Criteria for Modelling and Mapping Critical Loads and Levels and Air Pollution Effects, Risks and Trends: Chapter III Mapping Critical Levels for Vegetation, accessed via, http://icpvegetation.ceh.ac.uk/publications/documents/Chapter3-Mappingcriticallevelsforvegetation_000.pdf, 2017.

Collins, W. J., Sitch, S., and Boucher, O.: How vegetation impacts affect climate metrics for ozone precursors, Journal of Geophysical Research: Atmospheres, 115, D23308, 10.1029/2010JD014187, 2010.

Collins, W. J., Bellouin, N., Doutriaux-Boucher, M., Gedney, N., Halloran, P., Hinton, T., Hughes, J., Jones, C. D., Joshi, M., Liddicoat, S., Martin, G., O'Connor, F., Rae, J., Senior, C., Sitch, S., Totterdell, I., Wiltshire, A., and Woodward, S.: Development and evaluation of an Earth-System model – HadGEM2, Geosci. Model Dev., 4, 1051-1075, 10.5194/gmd-4-1051-2011, 2011.

Cooper, O. R., Parrish, D. D., Stohl, A., Trainer, M., Nedelec, P., Thouret, V., Cammas, J. P., Oltmans, S. J., Johnson, B. J., Tarasick, D., Leblanc, T., McDermid, I. S., Jaffe, D., Gao, R., Stith, J., Ryerson, T., Aikin, K., Campos, T., Weinheimer, A., and Avery, M. A.: Increasing springtime ozone mixing ratios in the free troposphere over western North America, Nature, 463, 344-348, http://www.nature.com/nature/journal/v463/n7279/suppinfo/nature08708_S1.html, 2010.

Cooper, O. R., Parrish, D., Ziemke, J., Balashov, N., Cupeiro, M., Galbally, I., Gilge, S., Horowitz, L., Jensen, N., and Lamarque, J.-F.: Global distribution and trends of tropospheric ozone: An observation-based review, Elementa: Science of the Anthropocene, 2, 000029, 2014.

Cox, P. M., Betts, R. A., Jones, C. D., Spall, S. A., and Totterdell, I. J.: Acceleration of global warming due to carbon-cycle feedbacks in a coupled climate model, Nature, 408, 184-187, 2000.

Cox, P. M.: Description of the TRIFFID dynamic global vegetation model, Hadley Centre technical note 24, 2001.

1106 Cruz, F. T., Pitman, A. J., and Wang, Y. P.: Can the stomatal response to higher atmospheric carbon
1107 dioxide explain the unusual temperatures during the 2002 Murray-Darling Basin drought?, Journal of
1108 Geophysical Research: Atmospheres, 115, 2010.
1109 de Arellano, J. V.-G., van Heerwaarden, C. C., and Lelieveld, J.: Modelled suppression of boundary-
1110 layer clouds by plants in a CO2-rich atmosphere, Nature geoscience, 5, 701-704, 2012.
1111 De Kauwe, M., Kala, J., Lin, Y.-S., Pitman, A., Medlyn, B., Duursma, R., Abramowitz, G., Wang, Y.-P.,
1112 and Miralles, D.: A test of an optimal stomatal conductance scheme within the CABLE land surface
1113 model, 8, 431-452, 2015.
1114 Derwent, R. G., Stevenson, D. S., Doherty, R. M., Collins, W. J., Sanderson, M. G., and Johnson, C. E.:
1115 Radiative forcing from surface NO x emissions: spatial and seasonal variations, Climatic Change, 88,
1116 385-401, 10.1007/s10584-007-9383-8, 2008.
1117 Derwent, R. G., Utembe, S. R., Jenkin, M. E., and Shallcross, D. E.: Tropospheric ozone production
1118 regions and the intercontinental origins of surface ozone over Europe, Atmospheric Environment,
1119 112, 216-224, https://doi.org/10.1016/j.atmosenv.2015.04.049, 2015.
1120 Ellsworth, D. S.: CO_2 enrichment in a maturing pine forest: are CO_2 exchange and water status in the
1121 canopy affected?, Plant, Cell and Environment, 22, 461-472, 1999.
1122 Emberson, L. D., Ashmore, M. R., Cambridge, H. M., Simpson, D., and Tuovinen, J.-P.: Modelling
1123 stomatal ozone flux across Europe, Environmental Pollution, 109, 403–413, 2000.
1124 Emberson, L. D., Simpson, D., Tuovinen, J.-P., Ashmore, M. R., and Cambridge, H. M.: Modelling and
1125 mapping ozone deposition in Europe, Water Air Soil Pollution, 130, 577–582, 2001.
1126 Emberson, L. D., Büker, P., and Ashmore, M. R.: Assessing the risk caused by ground level ozone to
1127 European forest trees: A case study in pine, beech and oak across different climate regions,
1128 Environmental Pollution, 147, 454–466, 2007.
1129 Engardt, M., Simpson, D., Schwikowski, M., and Granat, L.: Deposition of sulphur and nitrogen in
1130 Europe 1900-2050. Model calculations and comparison to historical observations, *Tellus B: Chem.*
1131 *Phys. Meteor.*, 69, 2017.
1132 Etheridge, D. M., Steele, L. P., Langenfelds, R. L., Francey, R. J., M., B., and Morgan, V. I.: Natural and
1133 anthropogenic changes in atmospheric CO2 over the last 1000 years from air in Antarctic ice and firn,
1134 Journal of Geophysical Research, 101(D2), 4115–4128, doi:10.1029/95JD03410, 1996.
1135 Fagnano, M., Maggio, A., and Fumagalli, I.: Crops' responses to ozone in Mediterranean
1136 environments, Environmental Pollution, 157, 1438-1444, 2009.
1137 Fares, S., Vargas, R., Detto, M., Goldstein, A. H., Karlik, J., Paoletti, E., and Vitale, M.: Tropospheric
1138 ozone reduces carbon assimilation in trees: estimates from analysis of continuous flux
1139 measurements, Global change biology, 19, 2427-2443, 2013.
1140 Felzer, B., Reilly, J., Melillo, J., Kicklighter, D., Sarofim, M., Wang, C., Prinn, R., and Zhuang, Q.: Future
1141 Effects of Ozone on Carbon Sequestration and Climate Change Policy Using a Global Biogeochemical
1142 Model, Climatic Change, 73, 345-373, 10.1007/s10584-005-6776-4, 2005.
1143 Felzer, B. S. F., Kicklighter, D. W., Melillo, J. M., Wang, C., Zhuang, Q., and Prinn, R. G.: Ozone effects
1144 on net primary productivity and carbon sequestration in the conterminous United States using a
1145 biogeochemistry model, Tellus, 56B, 230-248, 2004.
1146 Feng, Z., Kobayashi, K., and Ainsworth, E. A.: Impact of elevated ozone concentration on growth,
1147 physiology, and yield of wheat (Triticum aestivum L.): a meta-analysis, Global Change Biology, 14,
1148 2696-2708, 10.1111/j.1365-2486.2008.01673.x, 2008.
1149 Fowler, D., Flechard, C., Cape, J. N., Storeton-West, R. L., and Coyle, M.: Measurements of Ozone
1150 Deposition to Vegetation Quantifying the Flux, the Stomatal and Non-Stomatal Components, Water,
1151 Air, and Soil Pollution, 130, 63-74, 10.1023/a:1012243317471, 2001.
1152 Fowler, D., Pilegaard, K., Sutton, M., Ambus, P., Raivonen, M., Duyzer, J., Simpson, D., Fagerli, H.,
1153 Fuzzi, S., and Schjørring, J. K.: Atmospheric composition change: ecosystems–atmosphere
1154 interactions, Atmospheric Environment, 43, 5193-5267, 2009.

Franz, M., Simpson, D., Arneth, A., and Zaehle, S.: Development and evaluation of an ozone deposition scheme for coupling to a terrestrial biosphere model, Biogeosciences, 14, 45-71, doi:10.5194/bg-14-45-2017, 2017.

Friedlingstein, P., Cox, P., Betts, R., Bopp, L., von Bloh, W., Brovkin, V., Cadule, P., Doney, S., Eby, M., Fung, I., Bala, G., John, J., Jones, C., Joos, F., Kato, T., Kawamiya, M., Knorr, W., Lindsay, K., Matthews, H. D., Raddatz, T., Rayner, P., Reick, C., Roeckner, E., Schnitzler, K. G., Schnur, R., Strassmann, K., Weaver, A. J., Yoshikawa, C., and Zeng, N.: Climate–Carbon Cycle Feedback Analysis: Results from the C4MIP Model Intercomparison, Journal of Climate, 19, 3337-3353, 10.1175/jcli3800.1, 2006.

Fuhrer, J., Val Martin, M., Mills, G., Heald, C. L., Harmens, H., Hayes, F., Sharps, K., Bender, J., and Ashmore, M. R.: Current and future ozone risks to global terrestrial biodiversity and ecosystem processes, Ecology and Evolution, 6, 8785-8799, 10.1002/ece3.2568, 2016.

Gedney, N., Cox, P. M., Bett, R. A., Boucher, O., Huntingford, C., and Stott, P. A.: Detection of a direct carbon dioxide effect in continental river runoff records, Nature, 439, 835-838, 2006.

Gerosa, G., Marzuoli, R., Monteleone, B., Chiesa, M., and Finco, A.: Vertical Ozone Gradients above Forests. Comparison of Different Calculation Options with Direct Ozone Measurements above a Mature Forest and Consequences for Ozone Risk Assessment, Forests, 8, 337, 2017.

Grantz, D., Gunn, S., and VU, H. B.: O3 impacts on plant development: a meta-analysis of root/shoot allocation and growth, Plant, cell & environment, 29, 1193-1209, 2006.

Harmens, H., Mills, G., Emberson, L. D., and Ashmore, M. R.: Implications of climate change for the stomatal flux of ozone: A case study for winter wheat, Environmental Pollution, 146, 763-770, http://dx.doi.org/10.1016/j.envpol.2006.05.018, 2007.

Hayes, F., Wagg, S., Mills, G., Wilkinson, S., and Davies, W.: Ozone effects in a drier climate: implications for stomatal fluxes of reduced stomatal sensitivity to soil drying in a typical grassland species, Global Change Biology, 18, 948-959, 2012.

Heikkinen, J., Ketoja, E., Nuutinen, V., and Regina, K.: Declining trend of carbon in Finnish cropland soils in 1974–2009, Global Change Biology, 19, 1456-1469, 10.1111/gcb.12137, 2013.

Hofmockel, K. S., Zak, D. R., Moran, K. K., and Jastrow, J. D.: Changes in forest soil organic matter pools after a decade of elevated CO2 and O3, Soil Biology and Biochemistry, 43, 1518-1527, http://dx.doi.org/10.1016/j.soilbio.2011.03.030, 2011.

Hoshika, Y., Watanabe, M., Inada, N., and Koike, T.: Ozone-induced stomatal sluggishness develops progressively in Siebold's beech (Fagus crenata), Environmental Pollution, 166, 152-156, 2012a.

Hoshika, Y., Omasa, K., and Paoletti, E.: Whole-Tree Water Use Efficiency Is Decreased by Ambient Ozone and Not Affected by O3-Induced Stomatal Sluggishness, PLOS ONE, 7, e39270, 10.1371/journal.pone.0039270, 2012b.

Hoshika, Y., Watanabe, M., Inada, N., and Koike, T.: Model-based analysis of avoidance of ozone stress by stomatal closure in Siebold's beech (*Fagus crenata*), Annals of Botany, 112, 1149-1158, 2013.

Hoshika, Y., Katata, G., Deushi, M., Watanabe, M., Koike, T., and Paoletti, E.: Ozone-induced stomatal sluggishness changes carbon and water balance of temperate deciduous forests., Scientific Reports, doi:10.1038/srep09871, 2015.

Hurtt, G., Chini, L. P., Frolking, S., Betts, R., Feddema, J., Fischer, G., Fisk, J., Hibbard, K., Houghton, R., Janetos, A., and Jones, C. D.: Harmonization of land-use scenarios for the period 1500–2100: 600 years of global gridded annual land-use transitions, wood harvest, and resulting secondary lands, Climatic Change, 109, 117-161, 2011.

IGBP-DIS: International Geosphere-Biosphere Programme, Data and Information System, Potsdam, Germany. Available from Oak Ridge National Laboratory Distributed Active Archive Center, Oak Ridge, TN, ananilable at: http://www.daac.ornl.gov,

IPCC: Climate change 2013: The Physical Science Basis, IPCC Working Group I Contribution to AR5, 2013.

Jacobs, C. M. J.: Direct impact of atmospheric CO_2 enrichment on regional transpiration, Wageningen Agricultural University, 1994.

Janssens, I. A., Freibauer, A., Ciais, P., Smith, P., Nabuurs, G.-J., Folberth, G., Schlamadinger, B., Hutjes, R. W. A., Ceulemans, R., Schulze, E.-D., Valentini, R., and Dolman, A. J.: Europe's Terrestrial Biosphere Absorbs 7 to 12% of European Anthropogenic CO2 Emissions, Science, 300, 1538-1542, 10.1126/science.1083592, 2003.

Jones, C. D., Cox, P., and Huntingford, C.: Uncertainty in climate–carbon-cycle projections associated with the sensitivity of soil respiration to temperature, Tellus B, 55, 642-648, 10.1034/j.1600-0889.2003.01440.x, 2003.

Jung, M., Reichstein, M., Margolis, H. A., Cescatti, A., Richardson, A. D., Arain, M. A., Arneth, A., Bernhofer, C., Bonal, D., Chen, J., Gianelle, D., Gobron, N., Kiely, G., Kutsch, W., Lasslop, G., Law, B. E., Lindroth, A., Merbold, L., Montagnani, L., Moors, E. J., Papale, D., Sottocornola, M., Vaccari, F., and Williams, C.: Global patterns of land-atmosphere fluxes of carbon dioxide, latent heat, and sensible heat derived from eddy covariance, satellite, and meteorological observations, Journal of Geophysical Research: Biogeosciences, 116, n/a-n/a, 10.1029/2010JG001566, 2011.

Kala, J., De Kauwe, M. G., Pitman, A. J., Medlyn, B. E., Wang, Y. P., Lorenz, R., and Perkins-Kirkpatrick, S. E.: Impact of the representation of stomatal conductance on model projections of heatwave intensity., Scientific Reports, 1-7, 10.1038/srep23418, 2016.

Karlsson, P. E., Braun, S., Broadmeadow, M., Elvira, S., Emberson, L., Gimeno, B. S., Le Thiec, D., Novak, K., Oksanen, E., Schaub, M., Uddling, J., and Wilkinson, M.: Risk assessments for forest trees: The performance of the ozone flux versus the AOT concepts, Environmental Pollution, 146, 608-616, http://dx.doi.org/10.1016/j.envpol.2006.06.012, 2007.

Karnosky, D., Percy, K. E., Xiang, B., Callan, B., Noormets, A., Mankovska, B., Hopkin, A., Sober, J., Jones, W., and Dickson, R.: Interacting elevated CO2 and tropospheric O3 predisposes aspen (Populus tremuloides Michx.) to infection by rust (Melampsora medusae f. sp. tremuloidae), Global Change Biology, 8, 329-338, 2002.

Karnosky, D. F., Skelly, J. M., Percy, K. E., and Chappelka, A. H.: Perspectives regarding 50years of research on effects of tropospheric ozone air pollution on US forests, Environmental Pollution, 147, 489-506, 2007.

Keeling, C. D., and Whorf, T. P.: Atmospheric CO2 records from sites in the SIO air sampling network. In Trends: A Compendium of Data on Global Change, Carbon Dioxide Information Analysis Center, Oak Ridge National Laboratory, Oak Ridge, Tenn., U.S.A. , 2004.

Kitao, M., Löw, M., Heerdt, C., Grams, T. E., Häberle, K.-H., and Matyssek, R.: Effects of chronic elevated ozone exposure on gas exchange responses of adult beech trees (Fagus sylvatica) as related to the within-canopy light gradient, Environmental Pollution, 157, 537-544, 2009.

Kjellström, E., Nikulin, G., Hansson, U., Strandberg, G., and Ullerstig, A.: 21st century changes in the European climate: uncertainties derived from an ensemble of regional climate model simulations, Tellus A, 63, 24-40, 2011.

Kubiske, M., Quinn, V., Marquardt, P., and Karnosky, D.: Effects of Elevated Atmospheric CO2 and/or O3 on Intra-and Interspecific Competitive Ability of Aspen, Plant biology, 9, 342-355, 2007.

Lamarque, J., Shindell, D. T., Josse, B., Young, P., Cionni, I., Eyring, V., Bergmann, D., Cameron-Smith, P., Collins, W. J., and Doherty, R.: The Atmospheric Chemistry and Climate Model Intercomparison Project (ACCMIP): overview and description of models, simulations and climate diagnostics, Geoscientific Model Development, 6, 179-206, 2013.

Langner, J., Engardt, M., Baklanov, A., Christensen, J. H., Gauss, M., Geels, C., Hedegaard, G. B., Nuterman, R., Simpson, D., and Soares, J.: A multi-model study of impacts of climate change on surface ozone in Europe, Atmospheric Chemistry and Physics, 12, 10423-10440, 2012a.

Langner, J., Engardt, M., and Andersson, C.: European summer surface ozone 1990–2100, Atmospheric Chemistry and Physics, 12, 10097-10105, 2012b.

Le Quéré, C., Moriarty, R., Andrew, R. M., Peters, G. P., Ciais, P., Friedlingstein, P., Jones, S. D., Sitch, S., Tans, P., Arneth, A., Boden, T. A., Bopp, L., Bozec, Y., Canadell, J. G., Chini, L. P., Chevallier, F.,

Cosca, C. E., Harris, I., Hoppema, M., Houghton, R. A., House, J. I., Jain, A. K., Johannessen, T., Kato, E., Keeling, R. F., Kitidis, V., Klein Goldewijk, K., Koven, C., Landa, C. S., Landschützer, P., Lenton, A., Lima, I. D., Marland, G., Mathis, J. T., Metzl, N., Nojiri, Y., Olsen, A., Ono, T., Peng, S., Peters, W., Pfeil, B., Poulter, B., Raupach, M. R., Regnier, P., Rödenbeck, C., Saito, S., Salisbury, J. E., Schuster, U., Schwinger, J., Séférian, R., Segschneider, J., Steinhoff, T., Stocker, B. D., Sutton, A. J., Takahashi, T., Tilbrook, B., van der Werf, G. R., Viovy, N., Wang, Y. P., Wanninkhof, R., Wiltshire, A., and Zeng, N.: Global carbon budget 2014, Earth Syst. Sci. Data, 7, 47-85, 10.5194/essd-7-47-2015, 2015.

Le Quéré, C., Andrew, R. M., Canadell, J. G., Sitch, S., Korsbakken, J. I., Peters, G. P., Manning, A. C., Boden, T. A., Tans, P. P., Houghton, R. A., Keeling, R. F., Alin, S., Andrews, O. D., Anthoni, P., Barbero, L., Bopp, L., Chevallier, F., Chini, L. P., Ciais, P., Currie, K., Delire, C., Doney, S. C., Friedlingstein, P., Gkritzalis, T., Harris, I., Hauck, J., Haverd, V., Hoppema, M., Klein Goldewijk, K., Jain, A. K., Kato, E., Körtzinger, A., Landschützer, P., Lefèvre, N., Lenton, A., Lienert, S., Lombardozzi, D., Melton, J. R., Metzl, N., Millero, F., Monteiro, P. M. S., Munro, D. R., Nabel, J. E. M. S., Nakaoka, S. I., O'Brien, K., Olsen, A., Omar, A. M., Ono, T., Pierrot, D., Poulter, B., Rödenbeck, C., Salisbury, J., Schuster, U., Schwinger, J., Séférian, R., Skjelvan, I., Stocker, B. D., Sutton, A. J., Takahashi, T., Tian, H., Tilbrook, B., van der Laan-Luijkx, I. T., van der Werf, G. R., Viovy, N., Walker, A. P., Wiltshire, A. J., and Zaehle, S.: Global Carbon Budget 2016, Earth Syst. Sci. Data, 8, 605-649, 10.5194/essd-8-605-2016, 2016.

Le Quéré, C., Andrew, R. M., Friedlingstein, P., Sitch, S., Pongratz, J., Manning, A. C., Korsbakken, J. I., Peters, G. P., Canadell, J. G., Jackson, R. B., Boden, T. A., Tans, P. P., Andrews, O. D., Arora, V. K., Bakker, D. C. E., Barbero, L., Becker, M., Betts, R. A., Bopp, L., Chevallier, F., Chini, L. P., Ciais, P., Cosca, C. E., Cross, J., Currie, K., Gasser, T., Harris, I., Hauck, J., Haverd, V., Houghton, R. A., Hunt, C. W., Hurtt, G., Ilyina, T., Jain, A. K., Kato, E., Kautz, M., Keeling, R. F., Klein Goldewijk, K., Körtzinger, A., Landschützer, P., Lefèvre, N., Lenton, A., Lienert, S., Lima, I., Lombardozzi, D., Metzl, N., Millero, F., Monteiro, P. M. S., Munro, D. R., Nabel, J. E. M. S., Nakaoka, S.-I., Nojiri, Y., Padín, X. A., Peregon, A., Pfeil, B., Pierrot, D., Poulter, B., Rehder, G., Reimer, J., Rödenbeck, C., Schwinger, J., Séférian, R., Skjelvan, I., Stocker, B. D., Tian, H., Tilbrook, B., van der Laan-Luijkx, I. T., van der Werf, G. R., van Heuven, S., Viovy, N., Vuichard, N., Walker, A. P., Watson, A. J., Wiltshire, A. J., Zaehle, S., and Zhu, D.: Global Carbon Budget 2017, Earth Syst. Sci. Data Discuss, in review, 2017.

Leuzinger, S., and Körner, C.: Water savings in mature deciduous forest trees under elevated CO_2, Global Change Biology, 13, 2498-2508, doi:10.1111/j.1365-2486.2007.01467.x, 2007.

Lin, Y.-S., Medlyn, B. E., Duursma, R. A., Prentice, I. C., Wang, H., Baig, S., Eamus, D., de Dios, V. R., Mitchell, P., and Ellsworth, D. S.: Optimal stomatal behaviour around the world, Nature Climate Change, 5, 459-464, 2015.

Lindroth, R. L.: Impacts of Elevated Atmospheric CO2 and O3 on Forests: Phytochemistry, Trophic Interactions, and Ecosystem Dynamics, Journal of Chemical Ecology, 36, 2-21, 10.1007/s10886-009-9731-4, 2010.

Logan, J. A., Staehelin, J., Megretskaia, I. A., Cammas, J. P., Thouret, V., Claude, H., De Backer, H., Steinbacher, M., Scheel, H. E., Stübi, R., Fröhlich, M., and Derwent, R.: Changes in ozone over Europe: Analysis of ozone measurements from sondes, regular aircraft (MOZAIC) and alpine surface sites, Journal of Geophysical Research, 117, 1-23, 2012.

Lombardozzi, D., Levis, S., Bonan, G., and Sparks, J. P.: Predicting photosynthesis and transpiration responses to ozone: decoupling modeled photosynthesis and stomatal conductance, Biogeosciences, 3113-3130, 2012.

Lombardozzi, D., Levis, S., Bonan, G., Hess, P. G., and Sparks, J. P.: The Influence of Chronic Ozone Exposure on Global Carbon and Water Cycles, Journal of Climate, 28, 292-305, 10.1175/jcli-d-14-00223.1, 2015.

Long, S. P., Ainsworth, E. A., Leakey, A. D. B., Nosberger, J., and Ort, D. R.: Food for Thought: Lower-Than-Expected Crop Yield Stimulation with Rising CO_2 Concentrations, Science, 312, 1918-1921, 10.1126/science.1114722, 2006.

1305   Löw, M., Herbinger, K., Nunn, A., Häberle, K.-H., Leuchner, M., Heerdt, C., Werner, H., Wipfler, P.,
1306   Pretzsch, H., and Tausz, M.: Extraordinary drought of 2003 overrules ozone impact on adult beech
1307   trees (Fagus sylvatica), Trees, 20, 539-548, 2006.
1308   Loya, W. M., Pregitzer, K. S., Karberg, N. J., King, J. S., and Giardina, C. P.: Reduction of soil carbon
1309   formation by tropospheric ozone under increased carbon dioxide levels., Nature, 425, 705-707,
1310   2003.
1311   Luyssaert, S., Abril, G., Andres, R., Bastviken, D., Bellassen, V., Bergamaschi, P., Bousquet, P.,
1312   Chevallier, F., Ciais, P., Corazza, M., Dechow, R., Erb, K. H., Etiope, G., Fortems-Cheiney, A., Grassi, G.,
1313   Hartmann, J., Jung, M., Lathière, J., Lohila, A., Mayorga, E., Moosdorf, N., Njakou, D. S., Otto, J.,
1314   Papale, D., Peters, W., Peylin, P., Raymond, P., Rödenbeck, C., Saarnio, S., Schulze, E. D., Szopa, S.,
1315   Thompson, R., Verkerk, P. J., Vuichard, N., Wang, R., Wattenbach, M., and Zaehle, S.: The European
1316   land and inland water CO_2, CO, CH_4 and N_2O balance between 2001 and 2005, Biogeosciences, 9,
1317   3357-3380, 10.5194/bg-9-3357-2012, 2012.
1318   Massman, W. J.: A review of the molecular diffusivities of H_2O, CO_2, CH_4, CO, O_3, SO_2, NH_3, N_2O,
1319   NO, and NO_2 in air, O_2 and N_2 near STP, Atmospheric Environment, 32, 1111-1127,
1320   http://dx.doi.org/10.1016/S1352-2310(97)00391-9, 1998.
1321   Matyssek, R., Wieser, G., Ceulemans, R., Rennenberg, H., Pretzsch, H., Haberer, K., Löw, M., Nunn,
1322   A., Werner, H., and Wipfler, P.: Enhanced ozone strongly reduces carbon sink strength of adult beech
1323   (Fagus sylvatica)–Resume from the free-air fumigation study at Kranzberg Forest, Environmental
1324   Pollution, 158, 2527-2532, 2010a.
1325   Matyssek, R., Karnosky, D., Wieser, G., Percy, K., Oksanen, E., Grams, T., Kubiske, M., Hanke, D., and
1326   Pretzsch, H.: Advances in understanding ozone impact on forest trees: messages from novel
1327   phytotron and free-air fumigation studies, Environmental Pollution, 158, 1990-2006, 2010b.
1328   McLaughlin, S. B., Nosal, M., Wullschleger, S. D., and Sun, G.: Interactive effects of ozone and climate
1329   on tree growth and water use in a southern Appalachian forest in the USA, New Phytologist, 174,
1330   109-124, 10.1111/j.1469-8137.2007.02018.x, 2007a.
1331   McLaughlin, S. B., Wullschleger, S. D., Sun, G., and Nosal, M.: Interactive effects of ozone and climate
1332   on water use, soil moisture content and streamflow in a southern Appalachian forest in the USA,
1333   New Phytologist, 174, 125-136, 10.1111/j.1469-8137.2007.01970.x, 2007b.
1334   Medlyn, B. E., Badeck, F. W., De Pury, D. G. G., Barton, C. V. M., Broadmeadow, M., Ceulemans, R.,
1335   De Angelis, P., Forstreuter, M., Jach, M. E., Kellomaki, S., Laitat, E., Marek, M., Philippot, S., Rey, A.,
1336   Strassemeyer, J., Laitinen, K., Liozon, R., Portier, B., Roberntz, P., Wang, K., and Jstbid, P. G.: Effects
1337   of elevated [CO_2] on photosynthesis in European forest species: a meta-analysis of model
1338   parameters, Plant, Cell & Environment, 22, 1475-1495, doi:10.1046/j.1365-3040.1999.00523.x, 1999.
1339   Medlyn, B. E., Barton, C. V. M., Broadmeadow, M. S. J., Ceulemans, R., De Angelis, P., Forstreuter,
1340   M., Freeman, M., Jackson, S. B., Kellomaki, S., Laitat, E., Rey, A., Roberntz, P., Sigurdsson, B. D.,
1341   Strassemeyer, J., Wang, K., Curtis, P. S., and Jarvis, P. G.: Stomatal conductance of forest species
1342   after long-term exposure to elevated CO_2 concentration: a synthesis, New Phytologist, 149, 247-264,
1343   2001.
1344   Medlyn, B. E., Duursma, R. A., Eamus, D., Ellsworth, D. S., Prentice, I. C., Barton, C. V., Crous, K. Y., de
1345   Angelis, P., Freeman, M., and Wingate, L.: Reconciling the optimal and empirical approaches to
1346   modelling stomatal conductance, Global Change Biology, 17, 2134-2144, 2011.
1347   Mercado, L. M., Bellouin, N., Sitch, S., Boucher, O., Huntingford, C., Wild, M., and Cox, P. M.: Impact
1348   of changes in diffuse radiation on the global land carbon sink, Nature, 458, 1014-1017,
1349   http://www.nature.com/nature/journal/v458/n7241/suppinfo/nature07949_S1.html, 2009.
1350   Mills, G., Hayes, F., Wilkinson, S., and Davies, W. J.: Chronic exposure to increasing background
1351   ozone impairs stomatal functioning in grassland species, Global Change Biology, 15, 1522-1533,
1352   2009.
1353   Mills, G., Pleijel, H., Braun, S., Büker, P., Bermejo, V., Calvo, E., Danielsson, H., Emberson, L.,
1354   Grünhage, L., Fernández, I. G., Harmens, H., Hayes, F., Karlsson, P.-E., and Simpson, D.: New stomatal

1355 flux-based critical levels for ozone effects on vegetation, Atmospheric Environment, 5064-5068,
1356 2011a.

1357 Mills, G., Hayes, F., Simpson, D., Emberson, L., Norris, D., Harmens, H., and BÜKer, P.: Evidence of
1358 widespread effects of ozone on crops and (semi-)natural vegetation in Europe (1990–2006) in
1359 relation to AOT40- and flux-based risk maps, Global Change Biology, 17, 592-613, 10.1111/j.1365-
1360 2486.2010.02217.x, 2011b.

1361 Mills, G., Harmens, H., Wagg, S., Sharps, K., Hayes, F., Fowler, D., Sutton, M., and Davies, B.: Ozone
1362 impacts on vegetation in a nitrogen enriched and changing climate, Environmental Pollution, 208,
1363 898-908, 2016.

1364 Norby, R. J., Wullschleger, S. D., Gunderson, C. A., Johnson, D. W., and Ceulemans, R.: Tree responses
1365 to rising CO_2 in field experiments: implications for the future forest, Plant, Cell and Environment, 22,
1366 683-714, 1999.

1367 Norby, R. J., DeLucia, E. H., Gielen, B., Calfapietra, C., Giardina, C. P., King, J. S., Ledford, J., McCarthy,
1368 H. R., Moore, D. J. P., Ceulemans, R., De Angelis, P., Finzi, A. C., Karnosky, D. F., Kubiske, M. E., Lukac,
1369 M., Pregitzer, K. S., Scarascia-Mugnozza, G. E., Schlesinger, W. H., and Oren, R.: Forest response to
1370 elevated CO2 is conserved across a broad range of productivity, Proc. Natl. Acad. Sci. U. S. A., 102,
1371 18052-18056, 10.1073/pnas.0509478102, 2005.

1372 Nunn, A. J., Reiter, I. M., Häberle, K.-H., Langebartels, C., Bahnweg, G., Pretzsch, H., Sandermann, H.,
1373 and Matyssek, R.: Response patterns in adult forest trees to chronic ozone stress: identification of
1374 variations and consistencies, Environmental Pollution, 136, 365-369, 2005.

1375 O'Connor, F. M., Johnson, C. E., Morgenstern, O., Abraham, N. L., Braesicke, P., Dalvi, M., Folberth,
1376 G. A., Sanderson, M. G., Telford, P. J., Voulgarakis, A., Young, P. J., Zeng, G., Collins, W. J., and Pyle, J.
1377 A.: Evaluation of the new UKCA climate-composition model – Part 2: The Troposphere, Geosci.
1378 Model Dev., 7, 41-91, 10.5194/gmd-7-41-2014, 2014.

1379 Paoletti, E., and Grulke, N. E.: Ozone exposure and stomatal sluggishness in different plant
1380 physiognomic classes, Environmental Pollution, 158, 2664-2671, 2010.

1381 Parrish, D. D., Law, K. S., Staehelin, J., Derwent, R., Cooper, O. R., Tanimoto, H., Volz-Thomas, A.,
1382 Gilge, S., Scheel, H. E., Steinbacher, M., and Chan, E.: Long-term changes in lower tropospheric
1383 baseline ozone concentrations at northern mid-latitudes, Atmos. Chem. Phys., 12, 11485-11504,
1384 10.5194/acp-12-11485-2012, 2012.

1385 Parrish, D. D., Law, K. S., Staehelin, J., Derwent, R., Cooper, O. R., Tanimoto, H., Volz-Thomas, A.,
1386 Gilge, S., Scheel, H. E., Steinbacher, M., and Chan, E.: Lower tropospheric ozone at northern
1387 midlatitudes: Changing seasonal cycle, Geophysical Research Letters, 40, 1631-1636, 2013.

1388 Percy, K. E., Awmack, C. S., Lindroth, R. L., Kubiske, M. E., Kopper, B. J., Isebrands, J., Pregitzer, K. S.,
1389 Hendrey, G. R., Dickson, R. E., and Zak, D. R.: Altered performance of forest pests under atmospheres
1390 enriched by CO2 and O3, Nature, 420, 403-407, 2002.

1391 Royal-Society: Ground-level ozone in the 21st century: future trends, impacts and policy
1392 implications, Science Policy Report 15/08, 2008.

1393 Samuelsson, P., Jones, C. G., Willén, U., Ullerstig, A., Gollvik, S., Hansson, U., Jansson, C., Kjellström,
1394 E., Nikulin, G., and Wyser, K.: The Rossby Centre Regional Climate model RCA3: model description
1395 and performance, Tellus A, 63, 4-23, 2011.

1396 Saxe, H., Ellsworth, D. S., and Heath, J.: Tree and forest functioning in an enriched CO_2 atmosphere,
1397 New Phytologist, 139, 395-436, doi:10.1046/j.1469-8137.1998.00221.x, 1998.

1398 Schulze, E.-D., Ciais, P., Luyssaert, S., Schrumpf, M., Janssens, I. A., Thiruchittampalam, B., Theloke, J.,
1399 Saurat, M., Bringezu, S., and Lelieveld, J.: The European carbon balance. Part 4: integration of carbon
1400 and other trace-gas fluxes, Global Change Biology, 16, 1451-1469, 2010.

1401 Schulze, E. D., Luyssaert, S., Ciais, P., Freibauer, A., Janssens, I. A., and et al.: Importance of methane
1402 and nitrous oxide for Europe's terrestrial greenhouse-gas balance, Nature Geosci, 2, 842-850,
1403 http://www.nature.com/ngeo/journal/v2/n12/suppinfo/ngeo686_S1.html, 2009.

Sicard, P., De Marco, A., Troussier, F., Renoua, C., Vas, N., and Paoletti, E.: Decrease in surface ozone concentrations at Mediterranean remote sites and increase in the cities, Atmospheric Environment, 79, 705-715, 2013.

Simpson, D., Benedictow, A., Berge, H., Bergström, R., Emberson, L. D., Fagerli, H., Flechard, C. R., Hayman, G. D., Gauss, M., and Jonson, J. E.: The EMEP MSC-W chemical transport model–technical description, Atmospheric Chemistry and Physics, 12, 7825-7865, 2012.

Simpson, D., Andersson, C., Christensen, J. H., Engardt, M., Geels, C., Nyiri, A., Posch, M., Soares, J., Sofiev, M., and Wind, P.: Impacts of climate and emission changes on nitrogen deposition in Europe: a multi-model study, Atmospheric Chemistry and Physics, 14, 6995-7017, 2014a.

Simpson, D., Arneth, A., Mills, G., Solberg, S., and Uddling, J.: Ozone—the persistent menace: interactions with the N cycle and climate change, Current Opinion in Environmental Sustainability, 9, 9-19, 2014b.

Sitch, S., Cox, P. M., Collins, W. J., and Huntingford, C.: Indirect radiative forcing of climate change through ozone effects on the land-carbon sink, Nature, 448, 791-794, http://www.nature.com/nature/journal/v448/n7155/suppinfo/nature06059_S1.html, 2007.

Sitch, S., Friedlingstein, P., Gruber, N., Jones, S. D., Murray-Tortarolo, G., Ahlström, A., Doney, S. C., Graven, H., Heinze, C., Huntingford, C., Levis, S., Levy, P. E., Lomas, M., Poulter, B., Viovy, N., Zaehle, S., Zeng, N., Arneth, A., Bonan, G., Bopp, L., Canadell, J. G., Chevallier, F., Ciais, P., Ellis, R., Gloor, M., Peylin, P., Piao, S. L., Le Quéré, C., Smith, B., Zhu, Z., and Myneni, R.: Recent trends and drivers of regional sources and sinks of carbon dioxide, Biogeosciences, 12, 653-679, 10.5194/bg-12-653-2015, 2015.

Sleutel, S., De Neve, S., and Hofman, G.: Estimates of carbon stock changes in Belgian cropland., Soil Use and Management, 19, 166-171, 10.1079/SUM2003187, 2003.

Sun, G. E., McLaughlin, S. B., Porter, J. H., Uddling, J., Mulholland, P. J., Adams, M. B., and Pederson, N.: Interactive influences of ozone and climate on streamflow of forested watersheds, Global Change Biology, 18, 3395-3409, 10.1111/j.1365-2486.2012.02787.x, 2012.

Tai, P. K. A., Val Martin, M., and Heald, C. L.: Threat to future global food security from climate change and ozone air pollution, Nature Climate Change, 4, 817 - 821, 2014.

Talhelm, A. F., Pregitzer, K. S., Kubiske, M. E., Zak, D. R., Campany, C. E., Burton, A. J., Dickson, R. E., Hendrey, G. R., Isebrands, J. G., Lewin, K. F., Nagy, J., and Karnosky, D. F.: Elevated carbon dioxide and ozone alter productivity and ecosystem carbon content in northern temperate forests, Global Change Biology, 20, 2492-2504, 10.1111/gcb.12564, 2014.

Tans, P., and Keeling, R.: NOAA/ESRL (www.esrl.noaa.gov/gmd/ccgg/trends/), Scripps Institution of Oceanography (scrippsco2.ucsd.edu/). , 2014.

Tricker, P. J., Pecchiari, M., Bunn, S. M., Vaccari, F. P., Peressotti, A., Miglietta, F., and Taylor, G.: Water use of a bioenergy plantation increases in a future high CO_2 world, Biomass and Bioenergy, 33, 200-208, 2009.

Tuovinen, J.-P., Emberson, L., and Simpson, D.: Modelling ozone fluxes to forests for risk assessment: status and prospects, Annals of Forest Science, 66, 1-14, 2009.

Tuovinen, J., Hakola, H., Karlsson, P., and Simpson, D.: Air pollution risks to Northern European forests in a changing climate, Climate Change, Air Pollution and Global Challenges Understanding and Perspectives from Forest Research, 2013.

Uddling, J., Teclaw, R. M., Pregitzer, K. S., and Ellsworth, D. S.: Leaf and canopy conductance in aspen and aspen-birch forests under free-air enrichment of carbon dioxide and ozone, Tree Physiology, 29, 1367-1380, 2009.

van Vuuren, D. P., Edmonds, J., Kainuma, M., Riahi, K., Thomson, A., Hibbard, K., Hurtt, G. C., Kram, T., Krey, V., Lamarque, J.-F., Masui, T., Meinshausen, M., Nakicenovic, N., Smith, S. J., and Rose, S. K.: The representative concentration pathways: an overview, Climatic Change, 109, 5, 10.1007/s10584-011-0148-z, 2011.

Verstraeten, W. W., Neu, J. L., Williams, J. E., Bowman, K. W., Worden, J. R., and Boersma, K. F.: Rapid increases in tropospheric ozone production and export from China, Nature Geoscience 8, 690-695, 2015.

Vingarzan, R.: A review of surface ozone background levels and trends, Atmospheric Environment, 38, 3431-3442, https://doi.org/10.1016/j.atmosenv.2004.03.030, 2004.

Weedon, G. P., Gomes, S., Viterbo, P., Österle, H., Adam, J. C., Bellouin, N., Boucher, O., and Best, M. J.: The WATCH Forcing Data 1958-2001: a meteorological forcing dataset for land surface- and hydrological models. , WATCH Tech. Rep. 22, 41p (available at www.eu-watch.org/publications). 2010.

Weedon, G. P., Gomes, S., Viterbo, P., Shuttleworth, W. J., Blyth, E., Österle, H., Adam, J. C., Bellouin, N., Boucher, O., and Best, M.: Creation of the WATCH Forcing data and its use to assess global and regional reference crop evaporation over land during the twentieth century, Journal of Hydrometerology, 12, 823-848, doi: 10.1175/2011JHM1369.1., 2011.

Weedon, G. P.: Readme file for the "WFDEI" dataset.available at: http://www.eu-watch.org/gfx_content/documents/README-WFDEI.pdf, 2013.

Wild, O.: Modelling the global tropospheric ozone budget: exploring the variability in current models, Atmopsheric Chemistry and Physics, 2643–2660, 2007.

Wilkinson, S., and Davies, W. J.: Ozone suppresses soil drying-and abscisic acid (ABA)-induced stomatal closure via an ethylene-dependent mechanism, Plant, Cell & Environment, 32, 949-959, 2009.

Wilkinson, S., and Davies, W. J.: Drought, ozone, ABA and ethylene: new insights from cell to plant to community, Plant, Cell & Environment, 33, 510-525, 10.1111/j.1365-3040.2009.02052.x, 2010.

Wittig, V. E., Ainsworth, E. A., and Long, S. P.: To what extent do current and projected increases in surface ozone affect photosynthesis and stomatal conductance of trees? A meta-analytic review of the last 3 decades of experiments, Plant, Cell & Environment, 30, 1150-1162, 10.1111/j.1365-3040.2007.01717.x, 2007.

Wittig, V. E., Ainsworth, E. A., Naidu, S. L., Karnosky, D. F., and Long, S. P.: Quantifying the impact of current and future tropospheric ozone on tree biomass, growth, physiology and biochemistry: a quantitative meta-analysis, Global Change Biology, 15, 396-424, 10.1111/j.1365-2486.2008.01774.x, 2009.

Wullschleger, S. D., Gunderson, C. A., Hanson, P. J., Wilson, K. B., and Norby, R. J.: Sensitivity of stomatal and canopy conductance to elevated CO_2 concentration; interacting variables and perspectives of scale, New Phytologist, 153, 485-496, doi:10.1046/j.0028-646X.2001.00333.x, 2002.

Young, P., Arneth, A., Schurgers, G., Zeng, G., and Pyle, J. A.: The CO_2 inhibition of terrestrial isoprene emission significantly affects future ozone projections, Atmospheric Chemistry and Physics, 9, 2793-2803, 2009.

Young, P., Archibald, A., Bowman, K., Lamarque, J.-F., Naik, V., Stevenson, D., Tilmes, S., Voulgarakis, A., Wild, O., and Bergmann, D.: Pre-industrial to end 21st century projections of tropospheric ozone from the Atmospheric Chemistry and Climate Model Intercomparison Project (ACCMIP), Atmospheric Chemistry and Physics, 13, 2063-2090, 2013.

Zaehle, S.: Terrestrial nitrogen–carbon cycle interactions at the global scale, Philosophical Transactions of the Royal Society B: Biological Sciences, 368, 20130125, 10.1098/rstb.2013.0125, 2013.

Zak, D. R., Pregitzer, K. S., Kubiske, M. E., and Burton, A. J.: Forest productivity under elevated CO2 and O3: positive feedbacks to soil N cycling sustain decade-long net primary productivity enhancement by CO2, Ecology Letters, 14, 1220-1226, 10.1111/j.1461-0248.2011.01692.x, 2011.

1503

1504

1505

1506